Designing a combined Activation-Induced Marker and Intracellular Cytokine assay for comprehensive characterization of antigen-specific $CD4^+$ and $CD8^+$ T cells in SARS-CoV-2-infected children and adults

Yvonne Dogariu

Infection & Immunity

y.dogariu@students.uu.nl

Student number: 7019084

Utrecht University

La Jolla Institute for Immunology, La Jolla, California

Daily supervisor: Dr. Numana Bhat (nbhat@lji.org)

Examiner host institute: prof. Shane Crotty (shane@lji.org)

Examiner: assoc. prof. Monique Nijhuis (M.Nijhuis@umcutrecht.nl)

Abstract

The observation that children are at relatively lower risk of developing severe COVID-19 compared to adults has emerged early in the pandemic. However, no agreement has been reached as to whether pediatric SARS-CoV-2-specific humoral or cellular immune responses partly mediate clinical protection. Additionally, detailed knowledge of the development and maintenance of SARS-CoV-2-specific $CD4^+$ and $CD8^+$ T cells in children throughout the disease course is lacking. To best probe the SARS-CoV-2-specific T cell compartment, we have designed, optimized, and validated a hybrid AIM+ICS 24-color T cell spectral flow cytometry panel and protocol. We then demonstrated the suitability of the hybrid AIM+ICS for the comprehensive characterization of SARS-CoV-2-specific $CD4^+$ and $CD8^+$ T cell responses mounted by a subset of children and adults with mild or asymptomatic SARS-CoV-2 infection of the study cohort.

Laymen's summary

The emergence of the novel coronavirus has prompted tremendous research effort towards the understanding of protective immune mechanisms following SARS-CoV-2 infection. Broadly speaking, while multiple branches of the human immune system contribute to protection against SARS-CoV-2, most knowledge to date concerns the behavior of SARS-CoV-2-specific antibodies. This understanding has come to show that while antibodies generated post-infection are well-protective, they naturally diminish over time, and therefore recovered individuals are often left with insufficient levels of antibodies to altogether prevent re-infection. Thus, scientists have turned their attention towards other immune cell subsets which are better suited to contribute to protection against severe infection outcomes (that is, clinical protection) rather than altogether prevent reinfection. In this regard, T cells are a highly diverse immune cell subset with various roles in antiviral immunity; and while T cells are more difficult to study, SARS-CoV-2-specific T cells could offer the possibility of long-lasting protection following SARS-CoV-2 infection, and could even provide some degree of protection against emerging viral variants. Consequently, establishing the quantity and quality of SARS-CoV-2-specific T cells needed for clinical protection, as well as which disease settings (e.g., disease severities, patient groups, etc.) lead to the generation of these T cells have become important research avenues in recent times.

In this context, early studies throughout the pandemic have relied on more traditional techniques of identifying SARS-CoV-2-specific T cells, with the important drawback of a less precise assessment of the quantity of T cell responses. More recently, the technique called the *Activation-Induced Marker* (in short, "AIM") assay has been preferentially used because it allows a more accurate identification of SARS-CoV-2-specific T cells. However, this assay is rather laborious and costly, and offers only information regarding the *phenotype* (that is, the surface characteristics of cells) but not of the functional properties of the T cells analyzed. Therefore, in this study we used a hybrid version of the AIM assay, named in short "AIM+ICS", which allows the simultaneous assessment of both phenotype and function of SARS-CoV-2-specific T cells, thus allowing us to gain better insight into this immune cell subset.

Importantly, we optimized and applied this technique to allow the in-depth characterization of SARS-CoV-2 specific T cells of not only adult but also pediatric samples. Interestingly, children appear to be better protected against severe infection outcomes compared to adults. Still, the study of pediatric immune responses has so far been hindered by the limited blood volumes that can be obtained, which in turn allows relatively limited scientific insights to be obtained. In this context, our combined AIM+ICS assay is a very well-suited experimental technique to thoroughly analyze pediatric T cell responses following SARS-CoV-2 infection. Specifically, we inquired whether the quantity, quality, temporal development, or long-term maintenance of SARS-CoV-2-specific T cells are distinct in children with mild or asymptomatic SARS-CoV-2 infection compared to disease severity-matched adults. Thus, here we explored the link between SARS-CoV-2-specific T cells and the superior clinical protection of children following SARS-CoV-2 infection.

Introduction

T cells constitute an integral part of the human adaptive immune system and are a crucial line of defense against invading pathogens, with the critical ability of establishing long-term immunological memory. In the context of viral infections, several T cell subsets were shown to be essential in providing protection. Among these, $CD8^+$ T cells exert both direct and indirect cytotoxic functions by killing infected cells and/or secreting cytotoxic cytokines, respectively, whereas $CD4^+$ T cells orchestrate antiviral immunity in diverse ways. For instance, T follicular helper (Tfh) cells provide help to antigen (Ag)-specific B cells and thereby support the humoral immune response; T helper 1 (Th1) cells recognize intracellular pathogens and are largely responsible for the recruitment of other immune effector cells; lastly, $CD4^+$ cytotoxic lymphocytes (CD4-CTLs) possess the ability to release cytotoxic granules onto infected cells in a similar manner to $CD8^+$ T cells. Crucially, following infection resolution, a small subset of virus-specific $CD4^+$ and $CD8^+$ T cells differentiate into long-lasting, circulating or tissue resident memory T cells, which form the basis for rapid and potent anamnestic T cell responses against a subsequent (related) antigenic challenge (Brummelman et al., 2018). Thus, it is no surprise that both Ag-specific $CD4^+$ and $CD8^+$ T cells represent an invaluable immune component in providing clinical protection against SARS-CoV-2 infection as well. Importantly, emerging data show SARS-CoV-2-specific $CD4^+$ and $CD8^+$ T cells as an important correlate of protection with regards to disease severity (rather than infection acquisition) (Goldblatt et al., 2022); however, most evidence of T cell protection is indirect. First, the majority of SARS-CoV-2 infected individuals seroconvert and develop neutralizing antibodies that are detectable at 12 months post-infection, suggesting an effective germinal center response with potent $CD4^+$ Tfh cell-mediated help. Second, the high prevalence but relatively low titers of neutralizing antibodies in infected individuals at memory timepoints who nonetheless demonstrate good overall immunological memory and protection from (severe) SARS-CoV-2 reinfection together suggest a low likelihood of antibody-mediated sterilizing immunity that is likely offset by robust T cell-mediated protection. Third, a negative correlation has been observed between the magnitude of the SARS-CoV-2 specific $CD8^+$ T cell response and disease severity, suggesting that acute cytotoxic T cell responses are aptly able to control the ongoing SARS-CoV-2 infection, thereby limiting viral spread and consequent immunopathological damage. Lastly, SARS-CoV-2-specific $CD4^+$ and $CD8^+$ T cells have been shown to emerge in approximately ~100% and ~70% respectively of SARS-CoV-2-infected individuals across the disease severity spectrum, and to persist for longer than 8 months post-infection in most individuals (Sette & Crotty, 2022). Thus, potent T cell responses appear instrumental in improving clinical disease outcomes, shortening disease duration, as well as establishing robust long-term immunological memory, with possibly critical contributions for protective immunity particularly in the context of waning antibody levels and emerging viral variants. Briefly, SARS-CoV-2-specific T cell responses contribute to protection both in a direct cytotoxic fashion, as well as by supporting germinal center reactions and antibody generation (Goldblatt et al., 2022; Moss, 2022; Sette & Crotty, 2022). Nevertheless, while the importance of T cell immunity in SARS-CoV-2 infection is well recognized, the detailed examination of SARS-CoV-2-specific T cells has been hindered by the relative complexity and higher cost of the techniques needed for the comprehensive characterization of Ag-specific $CD4^+$ and $CD8^+$ T cells.

Historically, the identification of Ag-specific T cells has relied on the direct *ex vivo* interrogation of peptide-specific T cells using peptide-MHC multimers. This approach requires knowledge of peptide-HLA compatibility, and is limited by the diversity of HLA alleles in the human population, as well as by the multitude of peptides requiring interrogation to characterize a full Ag-specific $CD4^+$ and $CD8^+$ T cell response. In contrast, enzyme-linked immunospot (ELISpot) assays or the equivalent flow cytometry-based Intracellular Cytokine Staining (ICS) assays rely on *in vitro* stimulation with the target antigen, and antigen specificity is determined on the basis of cytokine secretion. However, the inherent heterogeneity of T cell populations prevents the use of solely one or few cytokines secreted in response to stimulation as a good proxy for the entire Ag-specific T cell response (Elias et al., 2020). In the context of the COVID-19 pandemic, it soon

became apparent that detailed knowledge of the phenotype, frequency, kinetics, and function of SARS-CoV-2-specific T cells was needed to enable a more complete understanding of T cell-mediated protection against SARS-CoV-2. In this regard, the activation-induced marker (AIM) assay has emerged in recent years as a tool to better capture Ag-specific $CD4^+$ and $CD8^+$ T cells, enabling a more extensive coverage of Ag-responsive T cells compared to peptide-MHC multimer-based assays, and with a higher sensitivity and specificity compared to cytokine-based assays (Dan et al., 2016; Reiss et al., 2017). The AIM assay relies on the detection of cell-surface activation markers (i.e. AIM markers), which are upregulated in a T cell receptor (TCR)-dependent manner following *in vitro* stimulation with (peptide pools of) the antigen of interest. Of note, much work has been done in the last two decades to elucidate the specificity of different AIM markers, their peak response in terms of length of *in vitro* culture, and the overlap of different AIM marker pairs in identifying the full breadth of Ag-responsive T cells for different antigens, allowing the utilization of the AIM assay for a range of antigens, disease/ vaccination settings, as well as downstream assays (Dan et al., 2016; Elias et al., 2020; Reiss et al., 2017). As such, AIM assays have served as an invaluable tool allowing the comprehensive assessment of Ag-specific $CD4^+$ and $CD8^+$ T cells in different infection and vaccination settings during the ongoing COVID-19 pandemic (Dan et al., 2021; Grifoni et al., 2020, 2021; Mateus et al., 2021; Moderbacher et al., 2020; Singh et al., 2022; Tarke et al., 2021; Tarke, Coelho, et al., 2022; Yu et al., 2022; Zhang et al., 2022). Importantly, a recent advance in the field of T cell immunology has been the development of a combined AIM and ICS assay (hereafter referred to as "AIM+ICS"), which allows the simultaneous interrogation of the phenotype, frequency, and kinetics of Ag-specific T cells using AIM marker expression, as well as of their functional profile via intracellular cytokine expression (Tarke, Coelho, et al., 2022; Tarke, Potesta, et al., 2022).

While the COVID-19 pandemic has brought an unprecedented, concerted global research effort towards the understanding of host immune responses against the novel SARS-CoV-2, most of this research has focused on adult populations, and thus relatively little is known about the immune response in infants, children and adolescents (hereon collectively referred to as 'children'). Interestingly, the observation that the pediatric population appears not to suffer as much from severe disease and hospitalization following SARS-CoV-2 infection as their adult counterparts emerged early in the pandemic (Dong et al., 2020; Liguoro et al., 2020; Ludvigsson, 2020). More recently, an epidemiological analysis of data collected in the European Union over the course of one year (August 2020 – October 2021) revealed that as little as 1.2% of children aged 0-17 years required hospitalization, 0.08% required ICU treatment, and only 0.01% died (Bundle et al., 2021). Likewise, it is well established that the majority of infections in children are asymptomatic or mildly symptomatic (Mansourian et al., 2021; Qi et al., 2021; Uzunoglu & Akca, 2021). Multiple hypotheses have been proposed with regards to the immunological differences that underlie the disease severity gap between children and adults following SARS-CoV-2 infection (Amodio et al., 2022; Brodin, 2022; Filippatos et al., 2021; Zimmermann & Curtis, 2022). Briefly, children appear to benefit from a timely and more robust interferon (IFN) response in airway immune and epithelial cells, likely allowing them to better restrict viral replication and spread early in infection (Yoshida et al., 2022). In addition, various studies have found lower frequencies of circulating cytotoxic T and NK cells, higher frequencies of regulatory T and B cells, and lower markers of pro-inflammatory cytokines in SARS-CoV-2-infected children; and therefore, children appear to be better equipped to resolve the inflammatory response following infection (Petrara et al., 2021; Yoshida et al., 2022). In support of this idea, both the innate and adaptive immune systems are more tolerogenic early in life, likely leading to a better balance between antiviral responses and unnecessary inflammation and subsequent tissue damage, with children displaying a lower intrinsic cytotoxicity of NK cells, higher frequencies of circulating regulatory T cells, higher frequencies of immunosuppressive erythroid precursor cells, and a T helper cell skewing away from the Th1 phenotype (Dowling & Levy, 2014; Hsieh et al., 2022). Moreover, the more naïve adaptive immune system of children, characterized by high frequencies of naïve $CD4^+$ and $CD8^+$ T cells and thus a larger proportion of unique TCR clones, likely stochastically enables a high-

affinity primary T cell immune response to occur in response to primary SARS-CoV-2 infection (Dowling & Levy, 2014; Yoshida et al., 2022). Overall, while the explanation for the disease severity gap observed between SARS-CoV-2 infected children and adults is likely multifactorial, the hypothesis that the early effective local control of infection together with the limited systemic immune activation and consequent immunopathology might account for the milder disease presentation in children raises the crucial question of whether children generate robust SARS-CoV-2-specific adaptive immune responses as well as potent and durable immunological memory in the absence of moderate to severe disease.

Given that the immune responses of children are more challenging to interrogate due to the scarcity of immune cells that can be harvested per child, as well as the relative difficulty of enrolling children in scientific studies, findings to date are based on data derived from fairly modest cohorts of SARS-CoV-2-infected children – in terms of overall sample size, as well as with regards to the inclusion of sufficient children across the age and disease severity spectrum, and temporally across the disease course. Despite these limitations, it is nevertheless apparent that at least a subset of SARS-CoV-2-infected children develop some degree of immunological memory in the absence of severe disease, with binding and neutralizing antibodies, as well as functional SARS-CoV-2-specific T cells (i.e. capable of secreting IFNg upon restimulation) being detected in numerous studies at various timepoints post-infection (Cohen et al., 2021; Dowell et al., 2022; Garrido et al., 2021; Kaaijk et al., 2022; Rowntree et al., 2022; Tian et al., 2022; Weisberg et al., 2021). Even so, most studies to date support a lower magnitude of SARS-CoV-2-specific T cells (Cohen et al., 2021; Kaaijk et al., 2022; Rowntree et al., 2022) in children relative to disease severity-matched adults, with greater waning of responses observed in recovered children (Kaaijk et al., 2022). Opposingly, only one study noted a durable SARS-CoV-2-specific T cell response of higher magnitude in infected children compared to adults (Dowell et al., 2022). Meanwhile, findings regarding antibody responses elicited by non-severe SARS-CoV-2 infection are more conflicting across studies, with several studies reporting either a lower (Kaaijk et al., 2022; Weisberg et al., 2021) or higher (Dowell et al., 2022) magnitude of anti-SARS-CoV-2 binding antibodies, as well as poorer (Weisberg et al., 2021) or greater (Garrido et al., 2021) levels of neutralizing antibodies in children compared to disease severity-matched adults; nevertheless, the durability of antibody responses was equally good in recovered children and adults across studies (Dowell et al., 2022; Kaaijk et al., 2022). Overall, while it is possible that such levels of SARS-CoV-2-specific antibodies and T cells are sufficient to contribute to protective immunity in children, more work is needed to ascertain how adaptive immune responses develop and are maintained in children following SARS-CoV-2 infection, as well as to understand the implications of differential adaptive immune responses in SARS-CoV-2-infected children relative to adults for the establishment of potent immunological memory.

This study is set to explore the link between the robustness of pediatric SARS-CoV-2-specific T cell responses and the superior clinical protection of children against SARS-CoV-2-infection. Specifically, we aim to closely examine the frequency, quality, kinetics, and function of SARS-CoV-2 specific $CD4^+$ and $CD8^+$ T cell responses in infants, children and adolescents over the course of asymptomatic or mild SARS-CoV-2 infection. We hypothesize that $CD4^+$ and/or $CD8^+$ T cells play a role in clinical protection, given several studies in adults that have shown that 1) an early T cell response of high breadth and magnitude is associated with a milder disease presentation; 2) robust memory SARS-CoV-2-specific T cell responses can also develop in the absence of antibodies in mild disease settings; and 3) higher magnitudes of SARS-CoV-2-specific Th1, circulating Tfh $CD4^+$ T cells, as well as $CD8^+$ T cells have been observed in mild disease compared to more severe disease settings (Lafon et al., 2021; Nelson et al., 2022; Sekine et al., 2020; Tan et al., 2021; Tarke, Potesta, et al., 2022). To best probe the SARS-CoV-2-specific T cell compartment, we have designed, optimized, and validated a hybrid AIM+ICS 24-color T cell spectral flow cytometry panel and protocol to allow comprehensive analysis of Ag-specific T cell responses mounted by SARS-CoV-2-infected children and disease severity-matched adults in our study cohort.

Results

24-color spectral flow cytometry T cell panel design for hybrid AIM+ICS assay

To comprehensively characterize Ag-specific $CD4^+$ and $CD8^+$ T cell responses in COVID-19-infected children and adults, here we have developed and optimized a 27-marker panel for spectral flow cytometry using 23 distinct fluorophores and one viability dye. The T cell panel includes T cell phenotyping markers CD3, CD4, CD8, and CXCR3 and CCR6 for T helper subset distribution; T cell memory markers CD45RA, CCR7, CD38 and CD27; T cell activation markers CD40L, CD69, 4-1BB, OX40, PD-1, and ICOS; T cell cytokine markers Tumor Necrosis Factor α (TNFa), interleukin 2 (IL-2), interleukin 10 (IL-10), interleukin 17 (IL-17), interferon γ (IFNg), and granzyme B (GzmB); dump markers CD14, CD16, and CD20 to allow the exclusion of non-T cell populations; and a viability dye to allow the exclusion of dead cells. The panel was designed using online resources provided by Cytek BioSciences (https://cytekbio.com/), such as the Cytek BioSciences Full Spectrum Viewer (https://spectrum.cytekbio.com), as well as based on information provided by the University of Chicago Cytometry and Antibody Technology Core Facility (https://voices.uchicago.edu/ucflow/).

Given that the majority of the markers of interest are 1) expressed on the same cell population (i.e. T cells), and 2) are upregulated in response to T cell activation (i.e. activation markers and cytokines), careful panel design was needed (see Table 1 for a panel overview). Given the high upregulation and inherent co-expression patterns of AIM markers following *in vitro* stimulation of cells, we prioritized AIM marker discrimination by assigning fluorophores that would have little spectral overlap and would not peak in the same emission channel. Importantly, since analysis of distinct pairs of AIM markers constitutes the main readout of the combined AIM+ICS hybrid assay, the following fluorophores were assigned: OX40 APC, CD40L PE-Dazzle594, CD69 FITC, and 41BB BV421, which have little spillover into one another, and thus would not lead to 'false positive' signal. This panel design strategy would also minimize 'false negative' signal, since the cross-spillover of AIM markers would require significant compensation to be applied, hence leading to loss of true AIM marker expression. Cytokine expression constitutes the second most important readout of the hybrid AIM+ICS, and often occurs at low frequencies by relatively rare cell populations; thus, bright fluorophores were assigned where possible, while minimizing spillover both between cytokine fluorophores, as well as from AIM marker fluorophores to cytokine fluorophores. The final panel design thus contains IFNg PE-Cy7, IL-10 BB700, IL-17 BV750, IL-2 BV650, TNFa eF450, and GzmB AF532. Furthermore, channels where spillover inevitably occurs ('drains into') from activation marker and cytokine fluorophores (which become highly expressed following *in vitro* stimulation and subsequent T cell activation) were assigned to T cell phenotyping markers that are stably expressed across T cell stimulation states, e.g. T cell subset and memory markers. These markers were also assigned dimmer fluorophores, and antibody titrations were optimized to reduce the mean fluorescence intensity of such highly, stably expressed T cell populations (e.g. $CD3^+$, $CD4^+$, $CD8^+$, or $CD45RA^+$ T cell subsets), in order to reduce overall 'noise' in the panel and unnecessary spread. Lastly, a dump channel was used in the BV510 fluorophore, which captures much of the spillover of the 24-color panel designed here; this panel design strategy is expected to not pose a problem since the population of interest is that resulting from negative gating. Similarly, the viability dye (Fixable Viability eF780) was chosen since it peaks in the infrared portion of the fluorescent spectrum, and as such, the bright signature of dying cells would not interfere with the remainder of the panel. Overall, the T cell spectral flow cytometry panel designed here has a relatively low complexity index of 7.19, where the complexity index is the overall spectral signature uniqueness of all the fluorophores included in a spectral flow cytometry panel, calculated using the online software https://spectrum.cytekbio.com; importantly, a lower complexity index indicates less spread and better resolution of the markers analyzed. Additionally, despite the use of a spectral flow cytometer (Cytek Aurora) which can discriminate highly similar fluorophores in terms of spectral signature, only few fluorophores included here have a very high similarity index (up to 0.85 similarity) and this relative panel simplicity was necessary to allow the proper discernment of the cell populations of interest given the

highly expressed nature of the markers included, and the significant upregulation of all markers of interest following T cell activation/stimulation (Fig. S1).

Laser	Marker	Fluorophore	Peak channel	Peak emission (nm)	Marker description
Ultraviolet	CD3	BUV395	UV2	395	Pan-T cell
	CCR6	BUV496	UV7	496	T helper cell subset
	ICOS	BUV563	UV9	563	Recent T follicular helper cell activation
	CD38	BUV661	UV11	661	Recent T cell memory subset
	PD-1	BUV737	UV14	737	T cell activation
	CD8	BUV805	UV16	805	T cell subset
Violet	41BB	BV421	V1	421	T cell activation
	TNFa	eF450	V3	450	Cytokine
	CD14 CD16 CD20	BV510	V7	510	Dump
	CD45RA	BV570	V8	570	T cell memory subset
	CXCR3	BV605	V10	602	T helper cell subset
	IL-2	BV650	V11	645	Cytokine
	CCR7	BV711	V13	711	T cell memory subset
	IL-17	BV750	V14	750	Cytokine
	CD27	BV785	V15	785	T cell memory subset
Blue	CD69	FITC	B2	525	T cell activation
	GzmB	AF532	B3	554	Cytokine
	IL-10	BB700	B9	695	Cytokine
Yellow-Green	CD40L	PE-Dazzle594	YG3	610	T cell activation
	IFNg	PE-Cy7	YG9	778	Cytokine
Red	OX40	APC	R1	660	T cell activation
	CXCR5	AF700	R3	719	T cell subset
	Viability	Fixable Viability eF780	R7	780	Viability
	CD4	APC-Fire810	R8	807	T cell subset

Table 1: Overview of 24-color spectral flow cytometry T cell panel, including spectral peak channel and peak emission wavelength per fluorophore, and marker description. *The following online software were used to describe fluorophore peak emission: https://app.fluorofinder.com/, and fluorophore peak spectral channel: https://cytekbio.com/ . Note that the marker description categories are not exhaustive.*

Hybrid AIM+ICS assay allows the sensitive detection of Ag-specific CD4$^+$ and CD8$^+$ T cells as well as cytokine expression

To determine whether the 24-color T cell panel developed here allowed specific and sensitive detection of Ag-specific CD4$^+$ and CD8$^+$ T cells and their cytokine expression profiles, a mix of COVID-19 convalescent and vaccinated donor PBMCs were analyzed in the hybrid AIM+ICS (n=6, of which 2 convalescent and 4 vaccinated donors). The gating strategy used for all optimization experiments for Ag-specific CD4$^+$ and CD8$^+$ T cells in the hybrid AIM+ICS is shown in Figure 1A. Ag-specific T cells were gated by examining two AIM markers simultaneously; the gates for each AIM marker pair within the CD4$^+$ and CD8$^+$ T cell compartments are shown in Figure 2A, and were drawn to best capture the AIM$^+$ population in the positive control wells while minimizing background AIM$^+$ expression in the negative control wells. Similarly, cytokine expression was determined by examining Cytokine$^+$ CD40L$^+$ cells within CD4$^+$ T cells, and Cytokine$^+$ CD69$^+$ cells within CD8$^+$ T cells; the gates for each of the six cytokines included in the panel are shown in Figure 2B. Spike megapool (MP) stimulation increased the frequency of AIM$^+$ CD4$^+$ T cells in all marker pairs relative to negative control (DMSO stimulation, Fig. 3A, left, $p<0.05$), and similar patterns of activation across all AIM marker pairs were observed following stimulation with the positive control SEB, although at a higher magnitude (Fig. 3A, right, $p<0.05$). Similarly, AIM$^+$ marker pairs within CD8$^+$ T cells showed varying degrees of upregulation following spike MP stimulation relative to DMSO baseline depending on the marker pair analyzed (Fig. 3B, left, $p<0.05$), and these patterns were preserved following SEB stimulation (Fig. 3B, right, $p<0.05$). Additionally, increases in intracellular cytokine production were detectable within both CD4$^+$ and

$CD8^+$ T cells following stimulation with either spike MP or SEB (Fig. 3C-D, respectively). As expected, different cytokine expression patterns emerged across the $CD4^+$ and $CD8^+$ T cell populations following Ag-specific stimulation (Fig. 3C-D, left), whereas a more similar (inflammatory cytokine) trend emerged in the $CD4^+$ and $CD8^+$ compartments following SEB stimulation (Fig. 3C-D, right). Importantly, limited IL-2, IL-10 and IL-17 production was detectable following spike MP stimulation in both the $CD4^+$ but particularly in the $CD8^+$ T cell population, reflecting the underlying functional polarization of the T cells analyzed. Overall, the hybrid AIM+ICS enabled the detection of increases in AIM^+ populations within both $CD4^+$ and $CD8^+$ compartments in an antigen-dependent fashion, as well as to capture T cell polarization and function by way of intracellular cytokine production.

Hybrid AIM+ICS assay improves the detection of Ag-specific $CD4^+$ and $CD8^+$ T cells

Given that the hybrid AIM+ICS assay could sensitively detect Ag-responsive T cells and their cytokine expression following *ex vivo* Ag-specific and -aspecific stimulation, we next inquired whether the hybrid AIM+ICS could detect Ag-specific $CD4^+$ and $CD8^+$ T cells as accurately as the golden standard for the assessment of Ag-specific T cell responses, i.e. the AIM assay. For this, we performed a head-to-head comparison on a mix of COVID-19 convalescent and vaccinee adult samples (n=11, of which 3 convalescent and 8 vaccinated donors). Briefly, PBMCs were stimulated for 22-24h with a SARS-CoV-2 Spike MP, or an equivalent amount of DMSO (negative control) or SEB (positive control). The following day, cells were either directly analyzed for activation marker expression in the AIM assay, or an additional 4h incubation containing Golgi Stop and Golgi Plug solutions was performed for the hybrid AIM+ICS, followed by surface staining and intracellular cytokine staining (see Methods for a detailed experimental overview). Importantly, all AIM marker antibodies were incubated together with the protein transport blocking mix, which was previously demonstrated by Tarke et al. (2022) to improve the detection of Ag-specific $CD4^+$ T cells in the hybrid assay in the case of 41BB (CD137). To best compare the two assays, antibody titrations were performed independently, and identical antibody concentrations were selected for T cell phenotypic and memory markers across the two assays – which were not expected to fluctuate due to the phenotypic stability of the markers as well as the similar staining methods across the two assays. Opposingly, higher antibody concentrations for activation markers were selected for the AIM assay compared to the AIM+ICS based on titration curves (data not shown); different antibody concentrations for AIM markers specifically were expected given the different staining techniques used in the two assays (surface staining in the AIM only vs 4h incubation in the AIM+ICS), and the longer overall duration of stimulation in the case of AIM+ICS. Representative flow plots for AIM^+ $CD4^+$ and $CD8^+$ T cells across stimulation conditions in the AIM only vs hybrid AIM+ICS assays are shown in Figure S2.

Within the $CD4^+$ T cell compartment, the hybrid AIM+ICS increased the baseline detection (DMSO stimulation condition) of the activation markers CD69, CD40L, and OX40 in all related marker pairs compared to AIM only ($p=0.001$ across all marker pairs, Fig. 4A, left), and this translated to an increase in the detection of Spike-specific $CD4^+$ T cells in the Spike MP-stimulated condition when examining the marker pairs $CD40L^+$ $CD69^+$, $OX40^+$ $CD40L^+$, and $OX40^+$ $CD69^+$ ($p=0.002$ across all marker pairs, Fig. 4A, middle). Opposingly, 41BB-related marker pairs showed a similar ($CD69^+$ $41BB^+$ and $OX40^+$ $41BB^+$) or lower ($CD40L^+$ $41BB^+$, $p=0.0333$) baseline detection in the hybrid AIM+ICS compared to AIM only (Fig. 4A, left), which translated to a generally lower detection of Spike-specific $CD4^+$ T cell responses in 41BB-related marker pairs in the hybrid assay (Fig. 4A, middle). Finally, similar stimulation indices were observed across all AIM marker pairs in the two assays (Fig. 4A, right). These results suggested that the 4h incubation of AIM markers (rather than surface stain) and/or the overall longer incubation time in the hybrid AIM+ICS contributed to the increased detection of Ag-specific $CD4^+$ T cells when defined as combinations of $CD40L^+$, $OX40^+$, or $CD69^+$ T cells. The hybrid AIM+ICS led to a diminished detection of Ag-specific $CD4^+$ T cells when analyzed as $41BB^+$ AIM^+ cells, possibly due to differential 41BB marker dynamics across the longer incubation time of the hybrid assay. Overall, the

hybrid AIM+ICS led to higher AIM$^+$ background levels, but also higher Spike-specific frequencies and similar stimulation indices of AIM$^+$ CD4$^+$ T cells compared to the AIM assay, demonstrating its suitability for the detection of Ag-specific CD4$^+$ T cells using canonical AIM CD4$^+$ markers such as CD40L, OX40 or CD69.

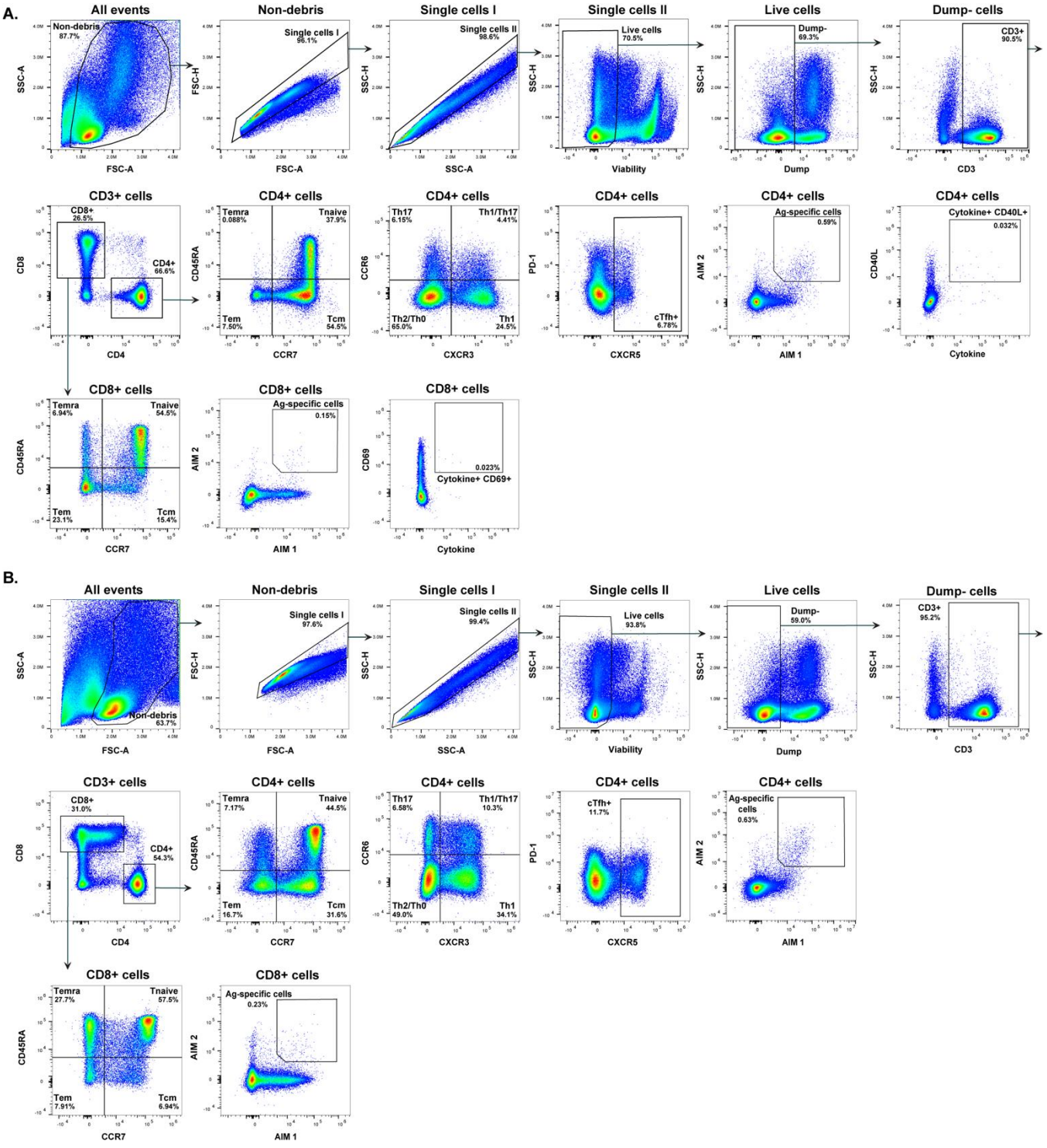

***Figure 1*: *Identification of Ag-specific CD4$^+$ and CD8$^+$ T cells by hybrid AIM+ICS or AIM assay*.** These gates were used for all optimization experiments, with slight variations to account for experiment-to-experiment variability; all the antibodies used were the same for all experiments, except for CD4, which was later changed to APC-Fire810 from PerCP-eF710. **A:** Representative gating strategy used for AIM+ICS hybrid assays. **B:** Representative gating strategy used for AIM assays. Note that different donors are shown in **A** and **B**.

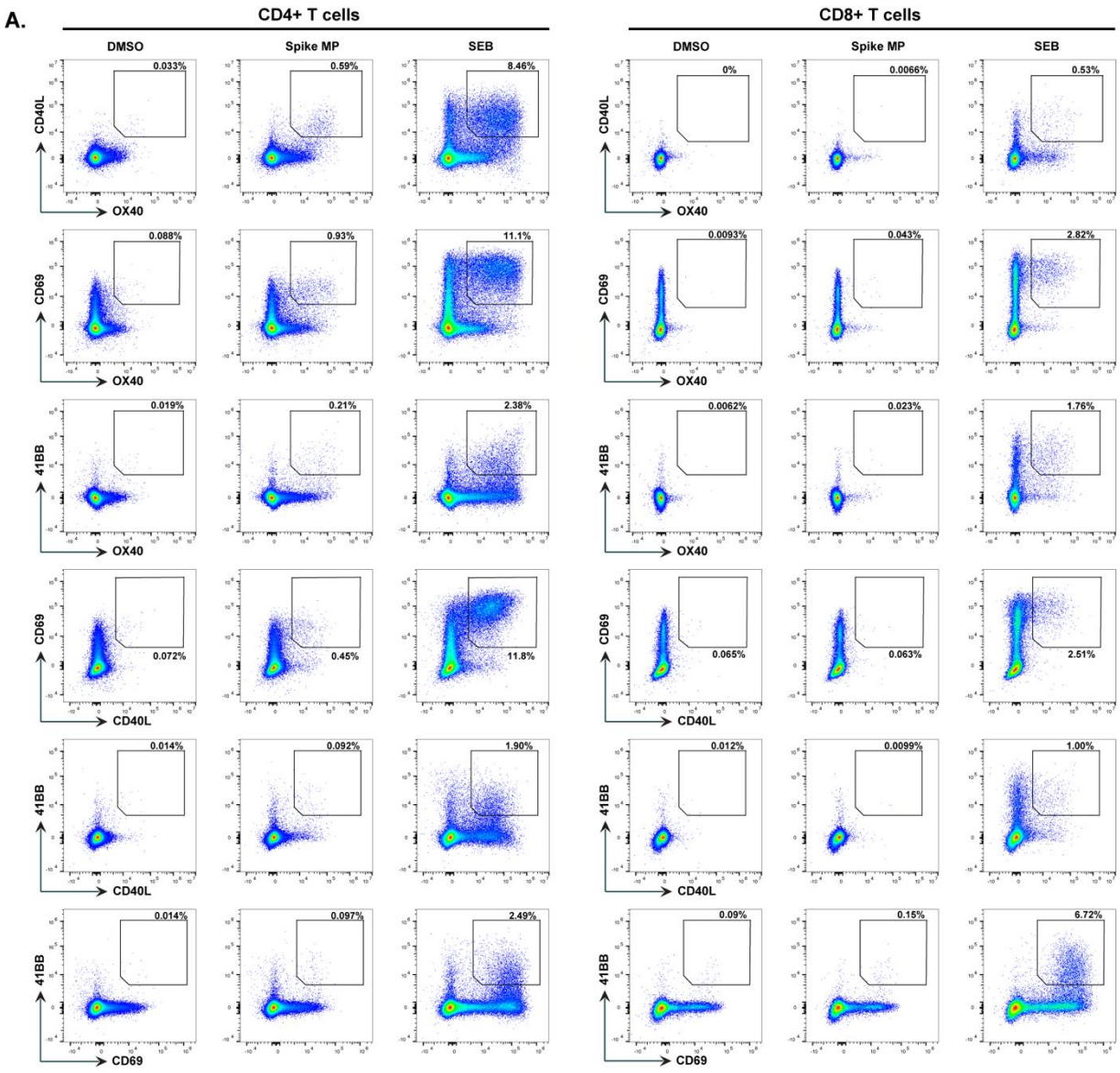

Figure 2 (legend and figure continued on following page)

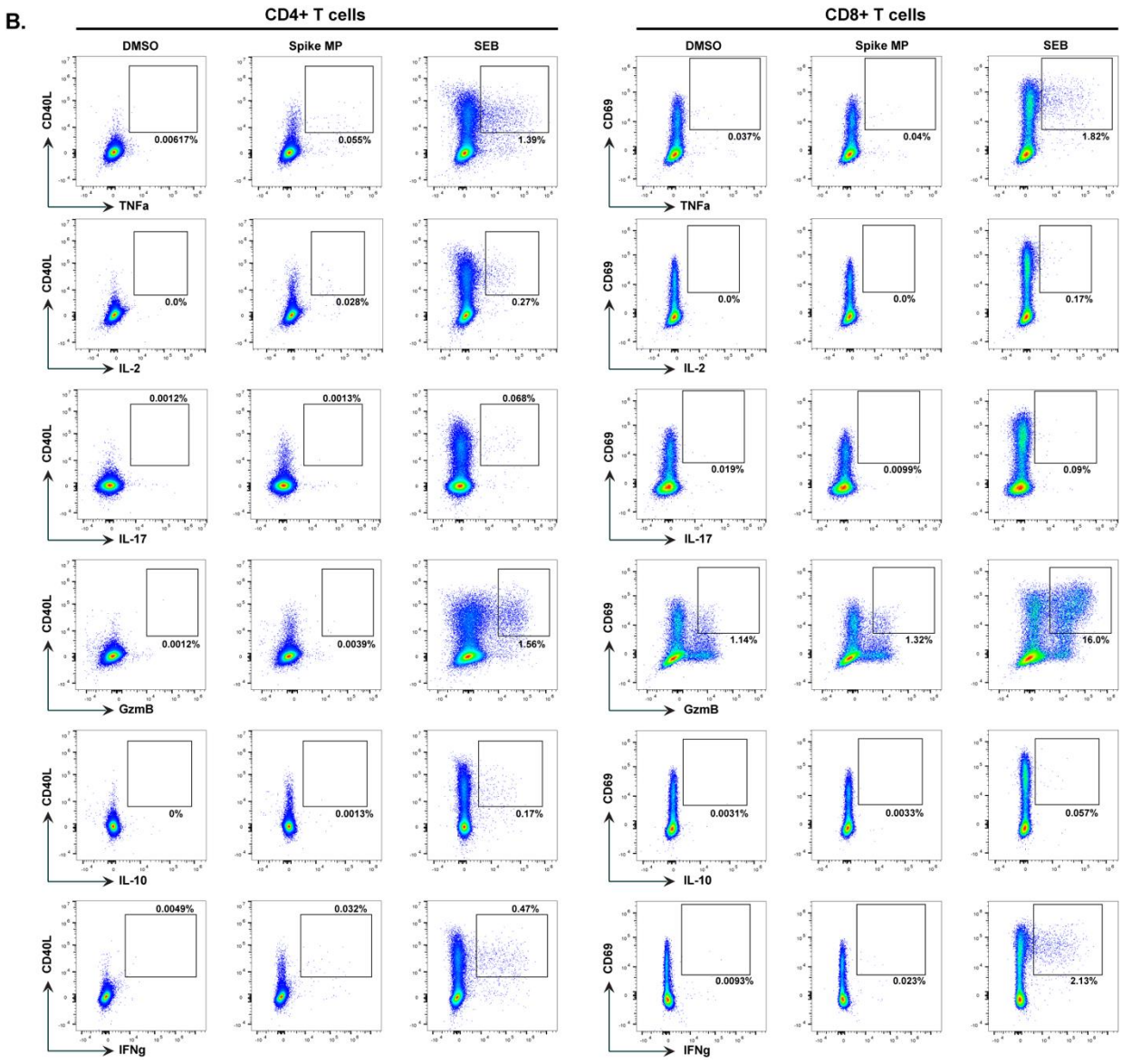

Figure 2: Representative gates used for the assessment of antigen specificity and cytokine production by CD4⁺ and CD8⁺ T cells in both hybrid AIM+ICS and AIM assays. These gates were used for all optimization experiments, with slight variations to account for experiment-to-experiment variability. **A**: Gating strategy for Ag-specific CD4⁺ (**left**) and CD8⁺ T cells (**right**) using two AIM markers simultaneously. (**B**) Gating strategy for cytokine production of CD4⁺ (**left**) and CD8⁺ T cells (**right**) using one AIM marker and one cytokine simultaneously. The same COVID-19 convalescent donor is shown in both **A** and **B**.

Within the CD8⁺ T cell compartment, the hybrid AIM+ICS enabled the detection of similar or higher frequencies of AIM⁺ CD8⁺ T cells following Spike MP stimulation across all marker pairs except OX40⁺ 41BB⁺ compared to AIM only (Fig. 4B, middle, $p>0.05$), whereas the baseline detection of activation markers was generally lower (for CD40L⁺ 41BB⁺, OX40⁺ CD40L⁺ and OX40⁺ CD69⁺ marker pairs, $p<0.05$) or similar between the hybrid AIM+ICS and AIM only assays (remaining AIM marker pairs, $p>0.05$, Fig. 4B, left). Similarly, the stimulation indices of Spike-specific CD8⁺ T cell responses were similar or higher across all AIM marker pairs in the hybrid AIM+ICS compared to AIM only ($p<0.01$ for OX40⁺ CD40L⁺ and OX40⁺ CD69⁺; remaining AIM marker pairs, $p>0.05$, Fig. 4B, right). Together, these findings indicated that the hybrid AIM+ICS appeared to improve the detection of Ag-specific CD8⁺ T cell responses, likely due to the longer incubation and/or different AIM marker staining technique utilized.

Interestingly, aspecific stimulation of T cells with SEB showed a uniform decrease in the frequency of both AIM⁺ CD4⁺ and CD8⁺ T cells in the hybrid AIM+ICS across all the marker pairs (Fig. 4C, $p<0.05$ for all AIM

marker pairs except OX40$^+$ CD69$^+$ within CD4$^+$ T cells), possibly reflecting the effects of the different biological pathways following Ag-specific or -aspecific T cell stimulation across the different timescales of the two assays.

Next, we examined whether the AIM+ICS hybrid assay behaves as reliably as the AIM assay when the same COVID-19 convalescent donor was analyzed across 3 independent experiments (Fig. S3). In terms of CD4$^+$ T cell responses, AIM$^+$ frequencies clustered strongly across different experiments with regards to DMSO, Spike MP, as well as SEB stimulation (n=2 and n=3 for AIM and AIM+ICS assays, respectively). CD8$^+$ T cell responses showed more variability within both AIM and AIM+ICS assays in the DMSO and Spike MP stimulation conditions, owing to the very low frequencies of Ag-responsive CD8$^+$ T cells, whereas the AIM$^+$ frequency following SEB stimulation clustered strongly across experiments in both assays. Thus, these results indicated the robust performance of the hybrid AIM+ICS in detecting AIM$^+$ CD4$^+$ and CD8$^+$ T cells across 3 independent experiments.

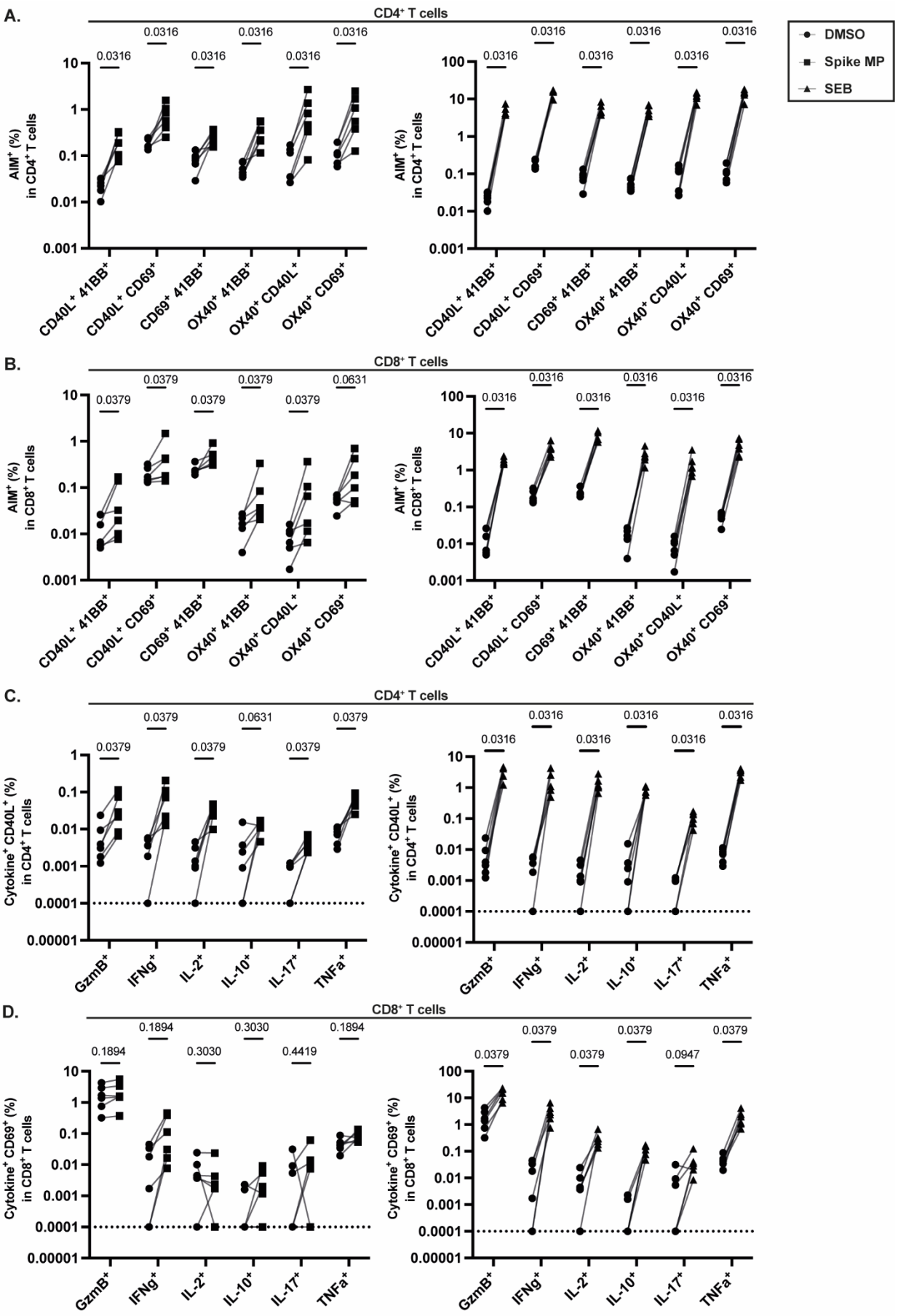
A.
CD4+ T cells
DMSO
Spike MP
SEB
AIM+ (%) in CD4+ T cells
CD40L+ 41BB+
CD40L+ CD69+
CD69+ 41BB+
OX40+ 41BB+
OX40+ CD40L+
OX40+ CD69+
B.
CD8+ T cells
AIM+ (%) in CD8+ T cells
C.
CD4+ T cells
Cytokine+ CD40L+ (%) in CD4+ T cells
GzmB+
IFNg+
IL-2+
IL-10+
IL-17+
TNFa+
D.
CD8+ T cells
Cytokine+ CD69+ (%) in CD8+ T cells

***Figure 3. Hybrid AIM+ICS allows detection of* AIM markers and cytokines**. **A-B**: Frequency of AIM$^+$ cells within the CD4$^+$ (**A**) or CD8$^+$ T cell compartment (**B**) following stimulation with spike MP (**left**) or SEB (**right**, positive control) relative to DMSO (negative control) stimulation. **C-D**: Frequency of Cytokine$^+$ CD40L$^+$ cells within the CD4$^+$ (**A**) or Cytokine$^+$ CD69$^+$ cells within the CD8$^+$ T cell compartment (**B**) following stimulation with spike MP (**left**) or SEB (**right**, positive control) relative to DMSO (negative control) stimulation. Dotted line indicates limit of detection. N=6; 2 COVID-19 convalescent and 4 vaccinated donors. Note that frequencies of AIM$^+$ cells (A-B) and Cytokine$^+$ AIM$^+$ cells (C-D) are shown prior to background subtraction across all stimulation conditions. Wilcoxon matched-pairs ranked sign test, with two-stage linear step-up procedure of Benjamini, Krieger and Yekutieli.

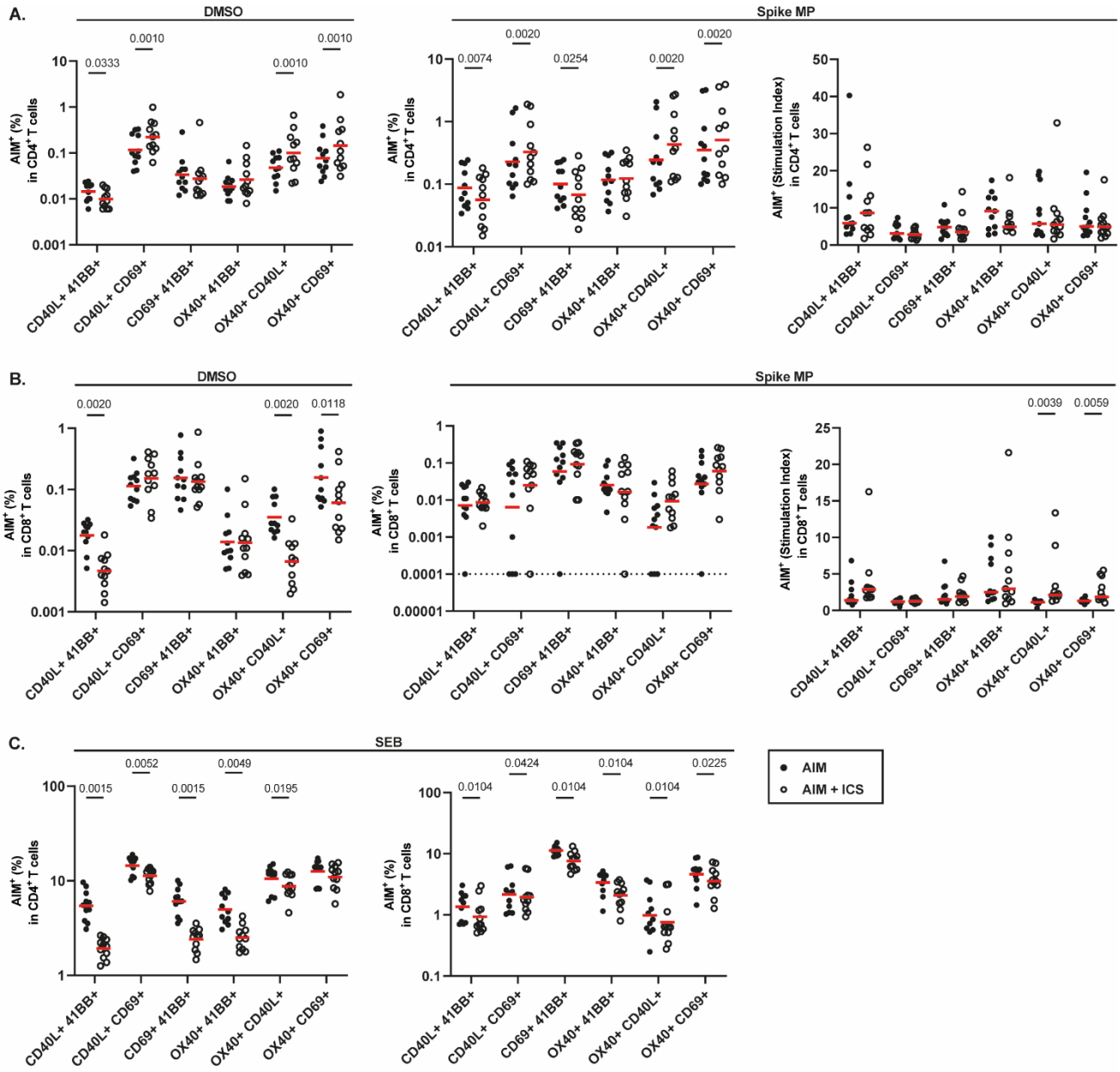

Figure 4: Head-to-head comparison of AIM and hybrid AIM+ICS assays. **A:** Frequency and stimulation indices of AIM$^+$ CD4$^+$ T cells following DMSO (**left**) or Spike MP (**middle** and **right**, respectively) in either AIM or AIM+ICS assays. **B:** Frequency and stimulation indices of AIM$^+$ CD8$^+$ T cells following DMSO (**left**), Spike MP (**middle** and **right**, respectively) in either AIM or AIM+ICS assays. **C**: Frequency of AIM$^+$ CD4$^+$ (**left**) and CD8$^+$ T cells (**right**) following SEB stimulation in either AIM or AIM+ICS assays. N=11; paired data; 3 COVID-19 convalescent and 8 vaccinated donors. Wilcoxon matched-pairs ranked sign test, with two-stage linear step-up procedure of Benjamini, Krieger and Yekutieli, only p>0.05 are shown. Dotted line indicates limit of detection.

Improved signal-to-noise ratio of Ag-specific CD4$^+$ T cells using decreased AIM antibody concentrations

Next, we set to improve the hybrid AIM+ICS assay to best capture Ag-specific CD4$^+$ and CD8$^+$ T cells while minimizing the detection of AIM$^+$ cells resulting from bystander activation (due to *in vitro* stimulation), pre-existing (*ex vivo*) activation, or aspecific staining. As observed in Figure 4, while the hybrid AIM+ICS captured more Ag-specific CD4$^+$ and CD8$^+$ T cells compared to the AIM assay, it also significantly increased the background detection of AIM$^+$ cells across CD40L$^+$ CD69$^+$, OX40$^+$ CD40L$^+$, and OX40$^+$ CD69$^+$ marker pairs within the CD4$^+$ T cell compartment. To improve the resolution of "true" AIM$^+$ (i.e. Ag-specific) CD4$^+$ T cells relative to baseline AIM$^+$ expression while not endangering the detection of AIM$^+$ CD8$^+$ T cells, we proceeded to optimize AIM marker antibody concentrations independently, depending on preferential AIM marker pairs used to identify Ag-specific CD4$^+$ and CD8$^+$ T cells. Given the importance of the AIM marker 41BB in identifying Ag-specific CD8$^+$ T cells (Dan et al., 2021; Mateus et al., 2021; Tarke et al., 2021; Tarke, Coelho, et al., 2022; Yu et al., 2022; Zhang et al., 2022), we decided to preserve the titration-curve derived antibody concentration; however, we proceeded to decrease CD69 and CD40L antibody concentrations, given their high contribution to background AIM$^+$ staining in the CD4$^+$ T cell compartment, as well as the rather aspecific nature of CD69 as an activation marker (Elias et al., 2020). Lastly, because of the relatively high specificity of OX40 as an AIM marker (Elias et al., 2020), we decided to preserve its titration curve-optimized antibody concentration. Hence, we analyzed the impact of preserving 41BB and OX40 antibody concentrations while simultaneously decreasing CD69 and CD40L antibody concentrations on the signal-to-noise ratio of AIM$^+$ CD4$^+$ and CD8$^+$ T cells.

To this end, we performed an AIM+ICS assay (n=6, of which 2 COVID-19 convalescent donors and 4 vaccinated donors) with either the titration curve-derived CD40L and CD69 antibody concentrations (hereafter referred to as "1x", i.e. CD40L 1:200 and CD69 1:100) or with 2.5x lower CD40L and CD69 antibody concentrations (i.e. CD40L 1:500 and CD69 1:250, hereafter referred to as "2.5x less"). As expected, the 2.5x less AIM+ICS panel led to 2.2 to 2.6-fold decreases in the geometric mean expression of AIM$^+$ CD4$^+$ T cells at baseline in all CD69-related marker pairs (Fig. 5A, top left, p=0.0631), with only 1.2- to 1.3-fold decreases in the geometric mean expression of the remaining AIM marker pairs (p>0.05). Following Spike MP stimulation, the 2.5x less AIM+ICS staining panel led to highly similar frequencies of AIM$^+$ CD4$^+$ T cells in the OX40$^+$ CD40L$^+$, OX40$^+$ 41BB$^+$, and CD40L$^+$ 41BB$^+$ marker pairs (Fig. 5A, top middle, p>0.9999), whereas 1.7-, 1.9-, and 2.6-fold decreases were observed in the OX40$^+$ CD69$^+$, CD40L$^+$ CD69$^+$, and CD69$^+$ 41BB$^+$ marker pairs, respectively (p=0.0631). Nevertheless, stimulation indices of Spike MP-stimulated CD4$^+$ T cells showed similar or higher levels across all AIM marker pairs with 2.5x less CD69 and CD40L antibody concentrations (Fig. 5A, top right, p>0.05), suggesting that the background expression of these AIM markers was overcontributing to the detection of Ag-specific CD4$^+$ T cells. Importantly, no significant decreases occurred in SEB-stimulated cells (Fig. 5A, bottom left, p>0.05), suggesting that the lower antibody concentrations were sufficient to saturate most AIM markers, even when expressed at high levels by a large fraction of the stimulated T cells. Within the CD8$^+$ T cell subset, background detection of AIM$^+$ CD8$^+$ T cells was mainly reduced in CD69-related marker pairs (Fig. 5B, top left, p>0.05), yet the stimulation indices of AIM$^+$ CD8$^+$ T cells were similar or higher across all AIM marker pairs following Spike MP stimulation (Fig. 5B, top right, p>0.05), suggesting no loss of 'true' Ag-specific CD8$^+$ T cells with lower CD69 and CD40L antibody concentrations. Similarly, highly similar frequencies of AIM$^+$ CD8$^+$ T cells were observed following SEB stimulation (Fig. 5B, bottom left, p>0.05). Overall, the lower CD40L and CD69 antibody concentrations appeared to support an improved detection of true Ag-specific CD4$^+$ T cells, while maintaining the detection of Ag-specific CD8$^+$ T cells.

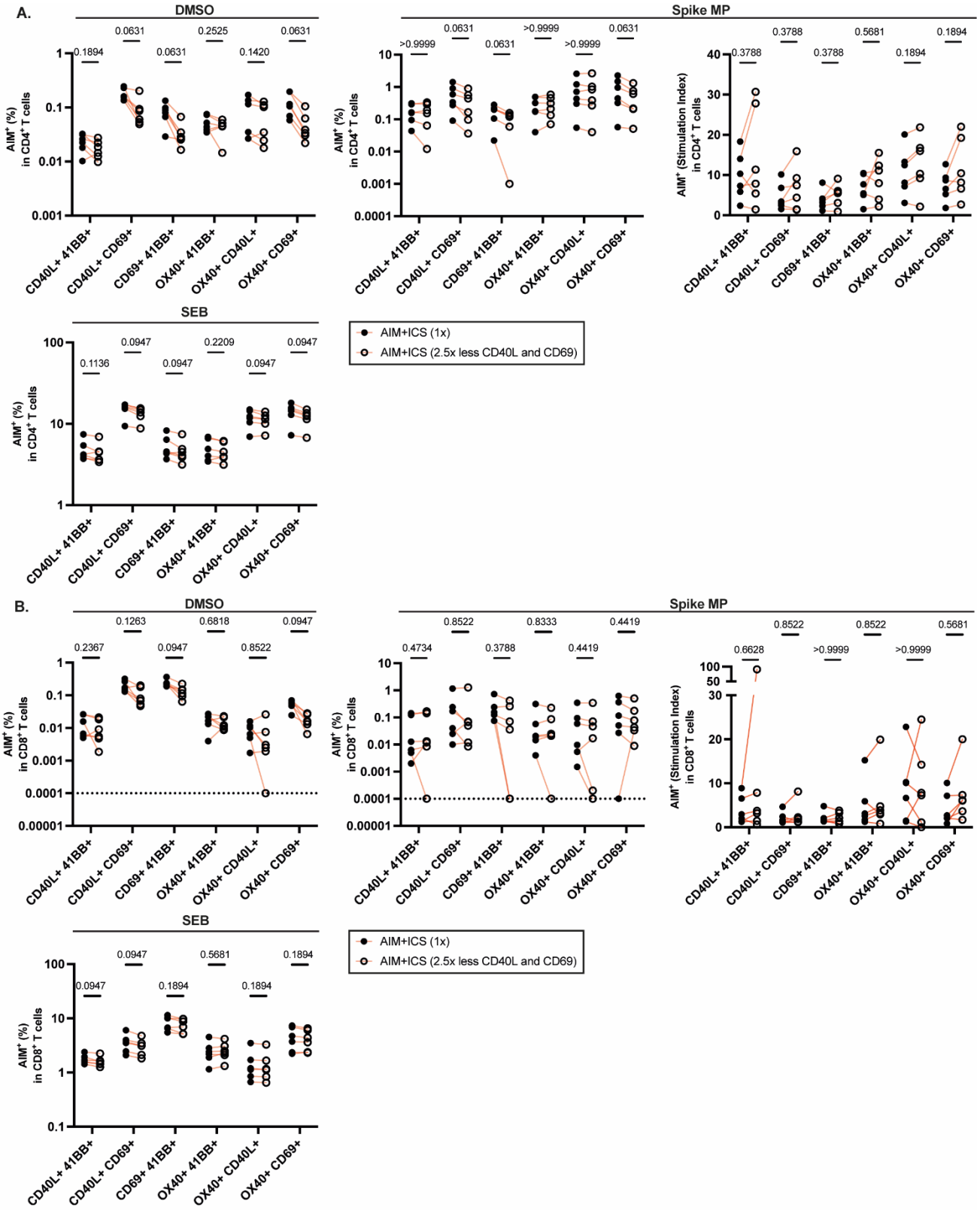

***Figure 5: Hybrid AIM+ICS with either titration curve-derived AIM antibody concentrations ("1x"), or decreased antibody concentrations of CD40L and CD69 ("2.5x less")*. A:** Frequency and stimulation indices of AIM⁺ CD4⁺ T cells following DMSO (**top left**), Spike MP (**top middle** and **right**, respectively), or SEB stimulation (**bottom**) stained with either "1x" or "2.5x less" CD40L and CD69 antibody concentrations within AIM+ICS. **B:** Frequency and stimulation indices of AIM⁺ CD8⁺ T cells following DMSO (**top left**), Spike MP (**top middle** and **right**, respectively), or SEB stimulation (**bottom**) stained with either "1x" or "2.5x less" CD40L and CD69 antibody concentrations within AIM+ICS. N=6; paired data; 2 COVID-19 convalescent and 4 vaccinated donors. Wilcoxon matched-pairs ranked sign test, with two-stage linear step-up procedure of Benjamini, Krieger and Yekutieli.

Optimized AIM+ICS panel detects Ag-specific $CD4^+$ and $CD8^+$ T cells in both adult and pediatric samples

Next, we assessed whether the optimized AIM+ICS panel could still detect Ag-specific $CD4^+$ and $CD8^+$ T cells in a sensitive and specific manner in an array of COVID-19 vaccinated and convalescent adult PBMC samples, as well as in SARS-CoV-2-infected pediatric samples from the study cohort. For this, we performed a head-to-head comparison of AIM and AIM+ICS assays, as previously described (n=10, of which 4 adult COVID-19 convalescent, 2 adult vaccinated, and 4 pediatric infected donors). The AIM+ICS led to an increase in the detection of AIM^+ $CD4^+$ T cells across all marker pairs in the DMSO stimulation condition (Fig. 6A, top left, $p<0.05$ for $CD40L^+$ $CD69^+$ and $OX40^+$ $CD40L^+$ marker pairs), with concurrent increases in the Spike MP stimulation condition (Fig. 6A, top middle, $p<0.05$ for all marker pairs except $CD69^+$ $41BB^+$ and $OX40^+$ $CD69^+$). In addition, stimulation indices of Spike MP-stimulated cells were similar across the two assays (Fig. 6A, top right, $p>0.05$), demonstrating the suitability of the hybrid AIM+ICS for the detection of SARS-CoV-2-specific $CD4^+$ T cells across a wide range of SARS-CoV-2-exposed adult and pediatric samples. In terms of SEB stimulation, the optimized hybrid AIM+ICS assay detected similar or lower frequencies of AIM^+ $CD4^+$ T cells when defined using the $CD40L^+$ $41BB^+$, $OX40^+$ $41BB^+$, and $CD69^+$ $41BB^+$ marker pairs (Fig. 6A, bottom, $p>0.05$), yet higher frequencies when defined as $CD40L^+$ $CD69^+$, $OX40^+$ $CD40L^+$, and $OX40^+$ $CD69^+$ marker pairs ($p<0.05$). This suggested that antibody concentrations in the hybrid AIM+ICS were still sufficient to stain AIM^+ $CD4^+$ T cells following SEB stimulation, with differences in AIM^+ expression between AIM and AIM+ICS assays being likely driven by assay-intrinsic causes (e.g. different incubation times and AIM staining techniques).

Within the $CD8^+$ T cell compartment, the hybrid AIM+ICS led to similar levels of AIM^+ $CD8^+$ T cells following DMSO stimulation (Fig. S4A, top left, $p>0.05$), yet similar or lower levels of AIM^+ $CD8^+$ T cells following Spike MP stimulation compared to the AIM assay (Fig. S4A, top middle, $p>0.05$ for $CD40L^+$ $CD69^+$, $OX40^+$ $CD40L^+$, $OX40^+$ $CD69^+$, and $OX40^+$ $41BB^+$ marker pairs, and $p<0.05$ for remaining AIM marker pairs). In addition, stimulation indices of Spike MP stimulated cells were not significantly different in the hybrid AIM+ICS compared to AIM only (Fig. S4A, top right, $p>0.05$). Nevertheless, SEB stimulation led to similar or higher levels of AIM^+ $CD8^+$ T cells within the hybrid AIM+ICS across most AIM marker pairs (Fig. S4A, bottom, $p<0.05$ for $CD40L^+$ $41BB^+$, $CD40L^+$ $CD69^+$, $OX40^+$ $CD40L^+$, $OX40^+$ $CD69^+$, and $OX40^+$ $41BB^+$ marker pairs), suggesting that the decrease in CD69 and CD40L antibody concentrations in the hybrid AIM+ICS did not endanger the ability of the hybrid AIM+ICS assay to capture AIM^+ expression within $CD8^+$ T cells. Thus, we concluded that despite the downregulation of CD69 and CD40L antibody concentrations, the optimized AIM+ICS assay was equally well-suited to the detection of SARS-CoV-2-specific $CD4^+$ and $CD8^+$ T cells as the golden standard AIM assay, and that the AIM+ICS hybrid assay allowed the detection of AIM^+ $CD4^+$ and $CD8^+$ T cells in both adults' as well as children's PBMCs.

To verify that the AIM and AIM+ICS assays identified highly similar populations of Ag-specific $CD4^+$ and $CD8^+$ T cells, we performed non-parametric Spearmen correlation analysis between AIM and AIM+ICS assays' detection of AIM^+ T cells following Spike MP stimulation. Importantly, the frequencies of SARS-CoV-2-specific $CD4^+$ T cells detected by the two assays strongly correlated across all marker pairs, with correlation coefficients ranging between 0.794 and 0.952 (Fig. 6B, top, $p<0.05$). Similarly, the two assays yielded highly correlated fold changes of AIM^+ $CD4^+$ T cells across all but one AIM marker pair, with correlation coefficients ranging between 0.830 and 0.988 (Fig. 6B, bottom, $p<0.05$ for all marker pairs except $OX40^+$ $41BB^+$). Similar trends emerged within the $CD8^+$ T cell compartment, with strongly correlated frequencies of SARS-CoV-2-specific $CD8^+$ T cells between the AIM and hybrid AIM+ICS assays (Fig. S4B, top, $p<0.05$, $r = 0.815$ to 0.960), and more modest correlations emerging in terms of fold change of SARS-CoV-2-specific $CD8^+$ T cells (Fig. S4B, bottom, $p<0.05$ for all marker pairs except $OX40^+$ $CD40L^+$). Thus, we concluded that the hybrid AIM+ICS assay

is well-suited to the detection of SARS-CoV-2-specific CD4⁺ and CD8⁺ T cells in both adult and pediatric samples, owing to its similar sensitivity and specificity to the golden standard AIM assay.

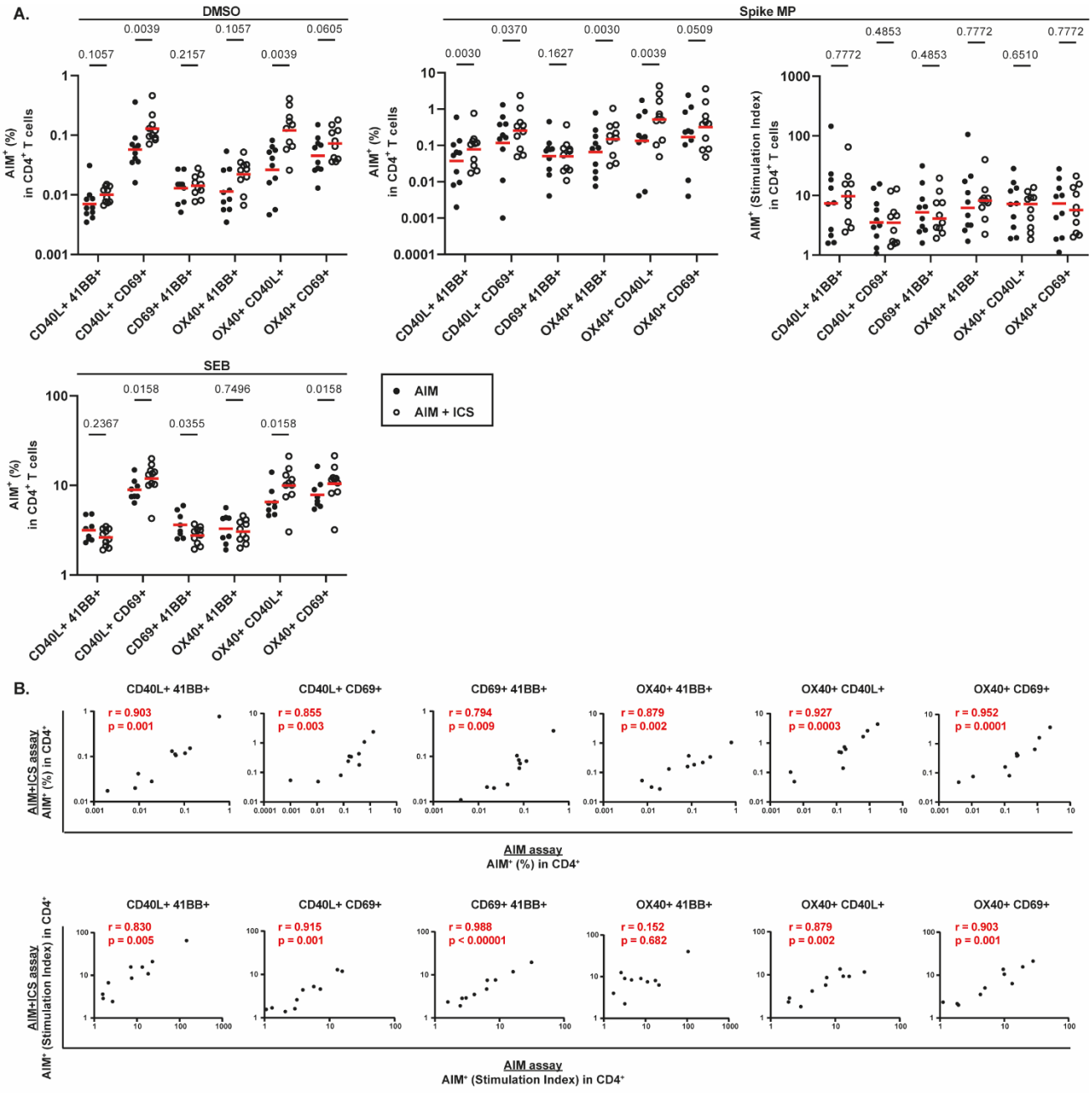

Figure 6: Head-to-head comparison of AIM and optimized hybrid AIM+ICS assays in adult and pediatric samples. **A:** Frequency and stimulation indices of AIM⁺ CD4⁺ T cells following DMSO (**top left**), Spike MP (**top middle** and **right**, respectively), or SEB stimulation (**bottom**) in either AIM or AIM+ICS assays. Wilcoxon matched-pairs ranked sign test, with two-stage linear step-up procedure of Benjamini, Krieger and Yekutieli. **B:** Frequency (**top**) and stimulation indices (**bottom**) of AIM⁺ CD4⁺ T cells following Spike MP stimulation displayed as correlations between AIM and AIM+ICS assays across AIM marker pairs. Correlation coefficients and P-values are shown following non-parametric Spearmen correlation analysis. N=10; paired data; 4 adult COVID-19 convalescent, 2 adult vaccinated, and 4 pediatric infected donors.

Preliminary analysis of SARS-CoV-2-specific CD4⁺ and CD8⁺ T cell responses in SARS-CoV-2-infected children and adults

To assess whether the optimized AIM+ICS is well-suited to the characterization of a diverse array of adult and pediatric samples representative of the entire study cohort, we performed a preliminary analysis of

SARS-CoV-2-specific $CD4^+$ and $CD8^+$ T cell responses in a heterogeneous subset of the study cohort (n=19 donors, of which 9 adults and 10 children, with multiple paired longitudinal samples per donor where available, leading to n=30 samples, of which 12 adults and 18 children). Figure S5 shows the distribution of paired samples per donor, timing post infection (days post symptom onset), donor age (years), as well as infection status. Of note, the inclusion of longitudinal samples per donor was necessary to later on minimize experimental differences while analyzing T cell kinetics data; however, the presence of paired samples might exacerbate underlying trends. Additionally, here we included 2 uninfected (i.e. SARS-CoV-2 PCR negative) children and adults each, and these donors were included in subsequent analyses as the magnitude of their SARS-CoV-2-specific T cell responses could potentially help discriminate between SARS-CoV-2-responders and non-responders among infected subjects. In terms of AIM+ICS methodology relative to the previous optimization experiments, here we also included a peptide pool containing experimentally defined epitopes of the non-Spike SARS-CoV-2 proteome (i.e., CD4 RE MP, see Methods) to interrogate the remainder of SARS-CoV-2-specific T cell responses in addition to Spike-specific T cell responses.

In terms of baseline $CD4^+$ T cell responses with DMSO, slightly higher frequencies of AIM^+ $CD4^+$ T cells were observed in SARS-CoV-2-infected adults relative to children across all AIM marker pairs (Fig. 7A, top left, $p>0.05$), suggesting inherent differences between groups in terms of *ex vivo* activation marker expression. Spike MP and CD4 RE MP stimulation led to similar frequencies of AIM^+ $CD4^+$ T cells across all AIM marker pairs in infected children compared to adults (Fig. 7A, top middle and right, $p>0.05$), likely due to the small sample size. SEB stimulation led to highly similar frequencies of AIM^+ $CD4^+$ T cells across groups (Fig. 7A, bottom, $p>0.05$), suggesting a similar responsiveness of adult and pediatric $CD4^+$ T cells to aspecific antigenic stimulation. Additionally, we calculated the stimulation indices of peptide-stimulated $CD4^+$ T cells across groups (Fig. 7B). While children showed slightly higher stimulation indices of Spike MP-stimulated $CD4^+$ T cells across all AIM marker pairs compared to adults (Fig. 7B, left, $p>0.05$), statistical significance was not reached. Likewise, CD4 RE-stimulated $CD4^+$ T cells demonstrated similar stimulation indices in infected children and adults (Fig. 7B, right, $p>0.05$). Furthermore, to define the proportion of adult and pediatric infected individuals that mounted detectable SARS-CoV-2-specific T cell responses for a certain SARS-CoV-2 peptide pool (i.e. responders), we used a stimulation index equal to or higher than 2 as cutoff for positive responses (this cutoff is shown in Figure 7B as a dotted line); importantly, this strategy takes into account baseline AIM marker expression per sample, and thus normalizes possible underlying differences in baseline AIM^+ responses across the two groups (Yu et al., 2022). Of note, more children mounted Spike-specific $CD4^+$ T cell responses compared to adults across all AIM marker pairs (Fig. 7C, top), and a similar trend emerged with regards to non-Spike-specific $CD4^+$ T cell responses, except for $CD40L^+$ $CD69^+$ (Fig. 7C, bottom). Thus, it appears that more infected children than adults included in this preliminary study mounted SARS-CoV-2-specific $CD4^+$ T cell responses of greater magnitude than the threshold of positivity, yet the analysis of the entire study cohort is needed to verify this trend.

Figure 7: Preliminary analysis of SARS-CoV-2-specific CD4⁺ T cell responses in 9 adults and 10 children. **A:** Frequency of AIM⁺ CD4⁺ T cells following DMSO (**top left**), Spike MP (**top middle**), CD4 RE MP (**top right**), or SEB stimulation (**bottom**). Mann-Whitney test; dotted line indicates the limit of detection. **B:** Stimulation indices of AIM⁺ CD4⁺ T cells following Spike MP (**left**) or CD4 RE MP stimulation (**right**) across AIM marker pairs. Dotted line indicates the threshold of positivity, where responses equal to or greater

than 2 are considered positive (i.e. SARS-CoV-2 responder). Mann-Whitney test. **C:** Pie charts showing the frequency of SARS-CoV-2 responders (defined as Stimulation index ≥2) to Spike MP (**top**) and CD4 RE MP (**bottom**) between adult and children cohorts. **D:** Frequency (**top**) and stimulation indices (**bottom**) of AIM$^+$ CD4$^+$ T cells displayed as correlations between Spike MP and CD4 RE MP-specific T cell responses. Correlation coefficients and P-values were calculated using non-parametric Spearmen correlation analysis. Adults are shown in black, and children are shown in orange; infection status is denoted by the relative size of the sample. N=30; 10 infected and 2 uninfected (SARS-CoV-2 PCR-negative) adult samples, 16 infected and 2 uninfected (SARS-CoV-2 PCR-negative) children samples. SI: Stimulation Index.

Next, we examined whether the magnitude of Spike-specific CD4$^+$ T cell responses correlates with non-Spike-specific CD4$^+$ T cell responses, which was previously observed in adult populations following natural infection (Yu et al., 2022). Indeed, both frequencies and stimulation indices of SARS-CoV-2-specific CD4$^+$ T cells revealed strong correlations between Spike MP and CD4 RE MP CD4$^+$ T cell responses across all adult and pediatric samples, with correlation coefficients varying between 0.737 and 0.908 for the frequency of AIM$^+$ CD4$^+$ T cells (Fig. 7D, top, $p<0.0001$), and between 0.845 and 0.897 for the stimulation indices of AIM$^+$ CD4$^+$ T cells (Fig. 7D, bottom, $p<0.0001$). Additionally, this correlation analysis could be used to determine whether SARS-CoV-2-uninfected donors included in the study cohort showed nonetheless detectable SARS-CoV-2-specific T cell responses following *ex vivo* restimulation with one or more peptide pools, or were true non-responders. For instance, it appears that only 1 out 2 uninfected adults and 1 out of 2 uninfected children included in the preliminary study were true non-responders, demonstrated by a stimulation index lower than 2 for both Spike MP and CD4 RE MP stimulation across most AIM marker pairs (Fig. 7D, bottom). Overall, this preliminary analysis shows that the AIM+ICS assay developed here can be used to accurately determine the infection status of both adult and pediatric SARS-CoV-2-infected individuals based on the fold change of the SARS-CoV-2-specific CD4$^+$ T cell response relative to DMSO baseline, as well as to sensitively quantify the magnitude of Ag-specific CD4$^+$ T cell responses in both children and adults.

While here we simultaneously presented the kinetics of all six AIM marker pairs, this analysis could also be used to assess the suitability of certain AIM marker pairs to best characterize SARS-CoV-2-specific CD4$^+$ T cells in infected children and adults, respectively, in our study cohort. First, it appears that AIM marker pairs follow a similar trend between children and adult groups across all stimulation conditions, though at different frequencies (Fig. 7A). Second, to assess the sensitivity of certain AIM marker pairs to recognize SARS-CoV-2-specific CD4$^+$ T cells, the rate of adult and pediatric responders (i.e. defined as Stimulation Index ≥2) detected by each AIM marker pair could be used (Fig. 7D). Thus, CD40L$^+$ 41BB$^+$ appears best suited to recognize both Spike-specific CD4$^+$ T cell responses, with a SARS-CoV-2 positivity rate of 26 out of 30 samples (86.67%), as well as CD4 RE-specific CD4$^+$ T cell responses, with a positivity rate of 25/30 (83.33%). Similarly, the OX40$^+$ 41BB$^+$ AIM marker pair appears second best suited for the detection of SARS-CoV-2-specific CD4$^+$ T cells in our study, with a positivity rate of 25/30 (83.33%) and 24/30 (80.00%) for Spike and non-Spike-specific CD4$^+$ T cell responses respectively. Lastly, the OX40$^+$ CD40L$^+$ AIM marker pair detected 21/30 responders (70.00%) following Spike MP stimulation, and 20/30 responders (66.67%) following CD4 RE MP stimulation. Overall, it appears that 1) the same AIM marker pair is equally suited to the detection of both Spike MP and CD4 RE MP-stimulated CD4$^+$ T cells, and 2) that the most sensitive AIM marker pairs - in the context of our study cohort and AIM+ICS protocol used - are highly dependent on baseline AIM marker expression. To exemplify, CD40L$^+$ 41BB$^+$ CD4$^+$ T cells showed the lowest frequency of all AIM marker pairs following DMSO stimulation, with only 0.012% and 0.007% AIM$^+$ CD4$^+$ T cells in adult and pediatric groups respectively; similarly, OX40$^+$ 41BB$^+$ and OX40$^+$ CD40L$^+$ demonstrated among the lowest background AIM marker expression in both cohorts (Fig. 7A, top left). Nevertheless, analysis of the entire study cohort will verify whether these AIM marker pairs will retain their sensitivity in the detection of adult and pediatric SARS-CoV-2-specific CD4$^+$ T cells analyzed this study.

Within the CD8$^+$ T cell compartment, DMSO stimulation led to similar or higher frequencies of AIM$^+$ CD8$^+$ T cells in infected children compared to infected adults (Fig. S6A, top left, $p<0.05$ for OX40$^+$ 41BB$^+$ and OX40$^+$ CD69$^+$, $p>0.05$ for remaining marker pairs). Similarly, children showed similar frequencies of AIM$^+$ CD8$^+$ T

cells following Spike MP stimulation compared to adults, apart from the $CD40L^+$ $CD69^+$ marker pair which showed a decreasing trend (Fig. S6A, top middle, $p<0.05$ for $CD40L^+$ $CD69^+$, $p>0.05$ for remaining marker pairs). Likewise, stimulation with the CD4 RE MP led to similar levels of AIM^+ $CD8^+$ T cells in infected children and adults (Fig. S6A, top right, $p>0.05$). Of note, SEB stimulation led to significantly lower levels of AIM^+ $CD8^+$ T cells in infected children when analyzed as $CD40L^+$ $41BB^+$, $CD40L^+$ $CD69^+$, or $OX40^+$ $CD40L^+$ $CD8^+$ T cells (Fig. S6A, bottom, $p<0.05$). Nevertheless, this trend appeared to be mainly driven by CD40L expression, since the remaining AIM marker pairs showed similar or higher levels of AIM^+ $CD8^+$ T cells in infected children relative to adults ($p>0.05$). Analysis of stimulation indices of Spike MP- and CD4 RE MP-stimulated $CD8^+$ T cells showed similar levels between children and adults, with a non-significant trend towards lower stimulation indices in infected children following CD4 RE MP stimulation compared to infected adults (Fig. S6B, $p>0.05$). Of note, very few adult and pediatric samples mounted an Ag-specific $CD8^+$ T cell response above the threshold of positivity (Stimulation Index ≥2) irrespective of peptide pool or AIM marker pair analyzed (Fig. S6B), and this translated to a low rate of SARS-CoV-2 responders with regards to the Ag-specific $CD8^+$ T cell compartment in both cohorts (Fig. S6C). Thus, in direct opposition to SARS-CoV-2-specific $CD4^+$ T cell responses, both adults and children mounted relatively poor $CD8^+$ T cell responses to both Spike and non-Spike stimulation, with overall more adults mounting detectable SARS-CoV-2-specific $CD8^+$ T cell responses relative to infected children when considering the trend emerging from all the AIM marker pairs. Despite the overall low frequency and stimulation indices of SARS-CoV-2-specific $CD8^+$ T cell responses, Spike MP- and CD4 RE MP-stimulated $CD8^+$ T cells still demonstrated moderate correlations across the adult and pediatric cohorts (Fig. S6D, $p<0.05$), suggesting that the sensitivity, rather than specificity, of the hybrid AIM+ICS in the detection of Ag-specific $CD8^+$ T cells is primarily affected. Nevertheless, the correlation analysis could not be used to discern the infection status within the $CD8^+$ T cell compartment, since both uninfected pediatric and adult samples largely fell within the cluster of low frequency SARS-CoV-2-specific $CD8^+$ T cell responses mounted by infected children and adults (Fig. S6D). Thus, it is likely that the AIM+ICS assay optimized for higher signal-to-noise ratio of AIM^+ $CD4^+$ T cell responses worsened the detection of SARS-CoV-2-specific $CD8^+$ T cells, which was reflected in the low frequency of Spike- and non-Spike-specific $CD8^+$ T cells in both infected adults and children, and in the low rate of responders irrespective of AIM marker pair.

In terms of suitable AIM marker pairs for the detection of SARS-CoV-2-specific $CD8^+$ T cell responses, the $CD40L^+$ $41BB^+$ marker pair detected the highest frequency of responders, with 15/30 (50%) and 13/30 (43.33%) of samples mounting responses above the threshold of positivity following Spike MP and CD4 RE MP stimulation respectively, followed by the $OX40^+$ $CD40L^+$ AIM marker pair, which detected 12/30 (40.00%) and 10/30 (33.33%) respectively. As for the $CD4^+$ T cell compartment, these trends seem rooted in the low background expression of AIM^+ $CD8^+$ T cells within these AIM marker pairs specifically, with as little as 0.004% expression of $CD40L^+$ $41BB^+$ $CD8^+$ T cells in both adult and pediatric groups, and 0.001% and 0.004% expression of $OX40^+$ $CD40L^+$ $CD8^+$ T cells respectively (Fig. S6A). Nevertheless, a larger sample size will be needed to ascertain these insights.

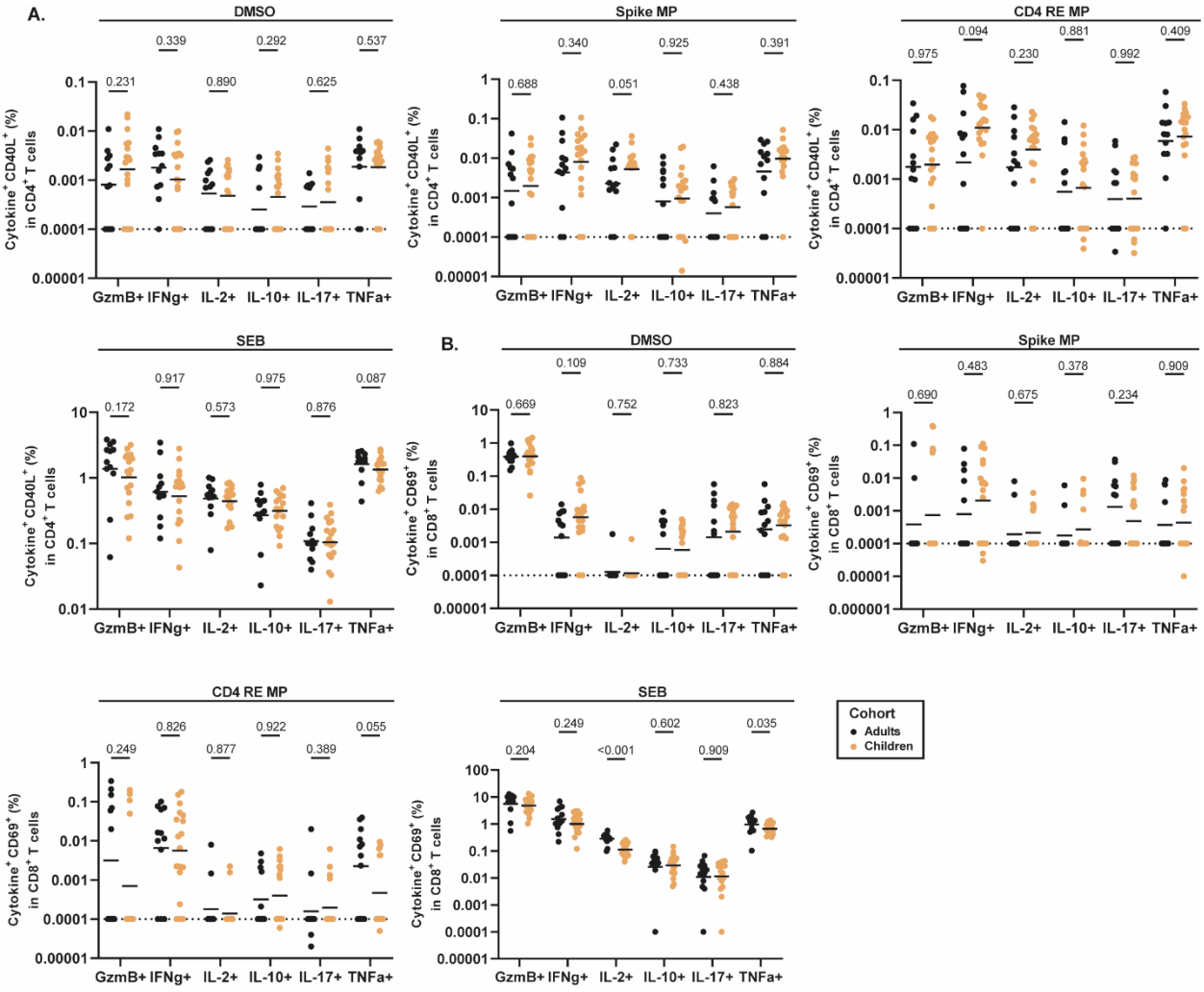

Figure 8: Preliminary analysis of cytokine expression by SARS-CoV-2-specific CD4⁺ and CD8⁺ T cells in 9 adults and 10 children. **A:** Frequency of Cytokine⁺ AIM⁺ CD4⁺ T cells following DMSO (**top left**), Spike MP (**top middle**), CD4 RE MP (**top right**), or SEB stimulation (**bottom**). Mann-Whitney test; dotted line indicates the limit of detection. **B:** Frequency of Cytokine⁺ AIM⁺ CD8⁺ T cells following DMSO (**top middle**), Spike MP (**top right**), CD4 RE MP (**bottom left**), or SEB stimulation (**bottom middle**). Mann-Whitney test; dotted line indicates the limit of detection. N=30; unpaired data; 10 infected and 2 uninfected (SARS-CoV-2 PCR-negative) adult samples, 16 infected and 2 uninfected (SARS-CoV-2 PCR-negative) children samples.

For cytokine expression analysis, we first determined the frequency of Cytokine⁺ CD40L⁺ cells within CD4⁺ T cells and Cytokine⁺ CD69⁺ cells within CD8⁺ T cells across stimulation conditions. Infected children and adults secreted slightly different levels of cytokines at baseline, with higher, though non-significant, levels of GzmB, IL-10, and IL-17 in infected children, and slightly lower levels of IFNg (Fig. 8A, top left, p>0.05). Interestingly, following Spike MP and CD4 RE MP stimulation, children mounted higher, though non-significant, levels of all six cytokines, with IL-2 expression showing the greatest difference in the Spike MP stimulation condition, and IFNg expression in the CD4 RE MP stimulation condition (Fig. 8A, top middle and right, p>0.05). Following SEB stimulation, children produced slightly lower levels of all cytokines except IL-10, with the strongest decrease observed in TNFa expression (Fig. 8A, bottom, p>0.05). Opposingly, pediatric CD8⁺ T cells showed higher expression of IFNg compared to adults at baseline, but highly similar expression of the remaining cytokines (Fig. 8B, top middle, p>0.05). Spike MP stimulation indicated a non-significant trend towards higher expression of GzmB, IFNg, IL-10, and TNFa within CD8⁺ T cells in infected children (Fig. 8B, top right, p>0.05), whereas CD4 RE MP stimulation led to more varied responses across the pediatric and adult groups, with slightly lower levels of GzmB and TNFa in infected children (Fig. 8B, bottom left, p>0.05). Once again, SEB stimulation revealed differences within the CD8⁺ T cell compartment between the adult and

pediatric cohorts, with decreases in IL-2 and TNFa expression in infected children (Fig. 8B, bottom middle, $p<0.05$). Importantly, analysis of the entire study cohort will be needed to verify whether these patterns will hold in a larger sample set, and to identify the cause or confounders contributing to certain differences.

To confirm that the trends emerging across groups were not primarily driven by differential AIM marker expression in children and adults, we next analyzed Cytokine$^+$ expression alone within CD4$^+$ and CD8$^+$ T cells respectively (Fig. S7); of note, the same cutoff for cytokine positivity was used when gating Cytokine$^+$ as well as Cytokine$^+$ AIM$^+$ T cells. Baseline expression of all 6 cytokines in CD4$^+$ T cells did not differ significantly across groups except for TNFa, which was produced at a lower frequency in children (Fig. S7A, top right, $p<0.05$ for TNFa, $p>0.05$ for remaining cytokines); of note, this trend was not apparent when cytokines were analyzed as Cytokine$^+$ CD40L$^+$. Subsequently, Spike MP and CD4 RE MP stimulation led to somewhat higher levels of all 6 cytokines within the CD4$^+$ T cell compartment in infected children rather than adults (Fig. S7A, top middle and right; $p<0.05$ for IL-2 expression within Spike MP stimulation condition, $p>0.05$ for remaining cytokines). This trend was also visible when cytokines were analyzed as Cytokine$^+$ CD40L$^+$, suggesting that SARS-CoV-2-specific CD4$^+$ T cells are more functional (i.e., more SARS-CoV-2-specific CD4$^+$ T cells are capable of cytokine production) in infected children than adults. Cytokine$^+$ expression within CD4$^+$ T cells following SEB stimulation showed similar patterns to the Cytokine$^+$ AIM$^+$ analysis (Fig. S7A, bottom, $p>0.05$), suggesting that the slightly lower cytokine trends visible in children are indeed driven by cytokine rather than AIM marker expression. Analysis of Cytokine$^+$ expression within CD8$^+$ T cells at baseline showed similar levels of all cytokines across groups except TNFa (Fig. S7B, top middle, $p>0.05$), which was not visible in the AIM$^+$ Cytokine$^+$ analysis. Spike MP and CD4 RE MP stimulation showed largely similar trends, with slightly lower GzmB production in children, but higher production of all other cytokines (Fig. S7B, bottom left, $p>0.05$). Lastly, SEB stimulation showed a very similar cytokine expression trend to the previous Cytokine$^+$ AIM$^+$ analysis (Fig. S7B, bottom middle, $p<0.05$ for IL-2 and TNF, $p>0.05$ for remaining cytokines). Overall, while the comparison of cytokine expression of SARS-CoV-2-specific CD4$^+$ and CD8$^+$ T cells in infected children and adults did not reveal statistically significant trends due to the low sample size, it is important to note that the intracellular cytokine analysis compensates for the relatively low sensitivity of the hybrid AIM+ICS assay in detecting Ag-specific CD8$^+$ T cells; this in turn underscores the importance of performing combined AIM and ICS analyses where possible.

Discussion

Here we developed and optimized a 24-color spectral flow cytometry T cell panel for a hybrid AIM+ICS assay to allow sensitive and accurate identification of Ag-specific $CD4^+$ and $CD8^+$ T cells, as well as their cytokine expression profiles (Table 1). We first showed that the hybrid AIM+ICS assay enables the detection in upregulation of activation markers on $CD4^+$ and $CD8^+$ T cells following the *ex vivo* Ag-specific and -aspecific stimulation of PBMCs (Fig. 3). Subsequently, we showed that the hybrid AIM+ICS performs equally well in identifying Ag-specific $CD4^+$ and $CD8^+$ T cells as the golden standard AIM assay (Fig. 4). Next, we optimized the signal-to-noise ratio of the hybrid AIM+ICS for the detection of true AIM^+ (i.e. Ag-specific) $CD4^+$ T cells while maintaining the detection of AIM^+ $CD8^+$ T cells by decreasing the antibody concentrations of several activation markers (Fig. 5-6 and S4). Lastly, we analyzed SARS-CoV-2-specific $CD4^+$ and $CD8^+$ T cell responses using the optimized hybrid AIM+ICS in a subset of SARS-CoV-2-infected children and adults from the study cohort (Fig. 7-8 and S6-7). Ultimately, given the preliminary analysis included only a small subset of the study cohort, we used this dataset to demonstrate the suitability of the hybrid AIM+ICS to sensitively detect underlying differences in the immune system composition and functionality of children and adults, as well as to identify differences in the phenotype, kinetics, magnitude, and function of SARS-CoV-2-specific $CD4^+$ and $CD8^+$ T cells in children and adults following infection.

The hybrid AIM+ICS affords several benefits compared to the AIM assay that has become the golden standard in recent years for the identification and detailed characterization of antigen-specific T cells in humans, mice, and non-human primates (Dan et al., 2016; Jiang et al., 2019; Reiss et al., 2017; Takahama et al., 2021). First, by combining an AIM assay with an Intracellular Cytokine Staining (ICS) assay, the hybrid AIM+ICS allows the simultaneous assessment of antigen specificity and cytokine expression of Ag-responsive T cells, thus gaining paired insight into the phenotypic and functional properties of Ag-specific T cells. Second, the hybrid AIM+ICS is advantageous relative to performing independent AIM and ICS assays because it allows the in-depth characterization of samples with reduced cell counts; this experimental technique will therefore allow the comprehensive characterization of Ag-specific T cell responses in immunological settings that were previously less amenable for research, such as children, immunocompromised, or severely sick individuals. Third, the hybrid AIM+ICS saves valuable time, labor, and reagents compared to performing independent AIM and ICS assays; this in turn will enable a larger proportion of immunology labs to perform in-depth Ag-specific T cell characterization. While we acknowledge that the number of fluorophores included in the panel proposed in this study would require a spectral analyzer, the principles behind the panel design as well as the relative panel simplicity would easily allow the transition to a conventional flow cytometer. Lastly, while we recognize that both AIM and AIM+ICS assays impose a higher cost and are more laborious compared to more traditional techniques for the identification of antigen-responsive T cells, we expect that the multitude of cell-based scientific insights that can be derived from performing a hybrid AIM+ICS assay will contribute to the progress of the SARS-CoV-2 pediatric T cell field.

Traditionally, several reasons have impeded the development of a combined AIM+ICS assay, such as the possible impact of fixation, permeabilization, and protein transport inhibition necessary for the characterization of intracellular cytokines on the sensitive detection of AIM markers. To overcome the expected negative impact of protein transport inhibition reagents on the surface detection of AIM markers, we adapted the typical AIM staining protocol to include a 4 hour incubation (rather than 30-60 minutes surface staining) of the AIM markers together with the protein transport inhibition mix, as first proposed for the detection of 41BB by Tarke et al. (2022). Given the dynamic nature of activation markers and their high turnover rates, we expected this staining strategy to increase the detection of AIM markers twofold, by allowing a longer (4h) time interval for staining, during which cells are still metabolically active (37°C rather than 4°C) and able to respond to the cognate antigen present in the cell culture; as well as by enabling the continuous staining of *de novo* expressed and recycled surface AIM markers. Importantly, we assumed the

internalized AIM marker-antibody complexes would contribute to the overall AIM$^+$ signal together with surface expressed AIM markers without the need for an additional intracellular AIM staining. To support our hypothesis, an early study addressed the effects of protein transport inhibition on the surface and intracellular expression of certain T cell markers, amongst which CD69; interestingly, they found that surface, but not intracellular, expression of CD69 was significantly diminished with the addition of brefeldin A, which is customarily used as (part of) a protein transport inhibition solution (O'Neil-Andersen & Lawrence, 2002). While other AIM markers were not directly addressed, we anticipated that similar effects might occur, and as such the AIM+ICS staining strategy utilized here of simultaneously adding AIM marker antibodies together with protein transport inhibition (rather than first blocking protein transport and then performing an AIM marker surface staining) was intended to partially counter these effects. Interestingly, the use of this staining strategy appeared to decrease the antibody concentrations needed to saturate AIM markers in the hybrid AIM+ICS compared to the concentrations typically used in the AIM assay; importantly, antibody concentrations derived from titration curves independently for both assays seemed to support this observation (data not shown). In turn, this observation prompted us to utilize different antibody concentrations for all the AIM markers when performing head-to-head comparisons across the two assays, with the premise that the best way to test the performance of the hybrid AIM+ICS would be when both assays are detecting the AIM markers as sensitively as possible. Importantly, despite the 1- to 4-fold lower AIM antibody concentrations, the AIM+ICS assay was able to detect higher frequencies of AIM$^+$ CD4$^+$ as well as CD8$^+$ T cells compared to the AIM assay across different stimulation conditions throughout the optimization experiments, suggesting that the AIM marker antibody concentrations used in the AIM+ICS were not undersaturated. Additionally, the various trends emerging in terms of differential AIM marker expression between the CD4+ and the CD8+ T cell compartments, as well as across the AIM and AIM+ICS assays, indicated a stronger impact of the underlying biology of the AIM markers across the two timescales and staining techniques of the two assays, as well as of the different stimulation conditions (DMSO, peptide megapool, and SEB) on AIM marker expression, rather than a clear negative impact of the AIM+ICS fixation, permeabilization, and protein transport inhibition. Overall, we concluded that the staining protocol proposed here enabled a specific and sensitive AIM marker detection within a hybrid AIM+ICS assay.

Interestingly, the hybrid AIM+ICS consistently showed higher background levels of most AIM marker pairs within the CD4$^+$ T cell compartment compared to the AIM assay (Fig. 4 and data not shown), which could potentially be attributed to the different AIM marker staining technique across the two assays, as well as the larger staining panel used in the AIM+ICS. To minimize the impact of background AIM$^+$ expression on the detection of true Ag-specific CD4$^+$ T cells, we proceeded to decrease AIM marker concentrations in order to reach a balanced signal-to-noise ratio (Fig. 5). In this regard, while we noticed a loss in background AIM$^+$ expression as well as a slight loss in the Spike-specific CD4$^+$ T cell response for certain AIM marker pairs, we preferentially relied on the stimulation indices of AIM$^+$ CD4$^+$ T cells across different AIM+ICS staining panels to assess whether we were detecting a larger proportion of true antigen-specific T cells relative to background AIM$^+$ T cells. Moreover, we used the frequency of AIM$^+$ T cells identified by different AIM+ICS staining panels following SEB stimulation as an indication of sufficient antibody concentrations when AIM markers are maximally expressed. Based on these considerations, we determined that the downregulation in CD40L and CD69 antibody concentrations 2.5-fold below the concentrations determined through antibody titration led to an optimal signal-to-noise ratio (Fig. 5). Surprisingly, we observed a diminished magnitude of SARS-CoV-2-specific CD8$^+$ T cell responses in the study cohort in both pediatric and adult samples (Fig. S4 and S6), given that previous optimization experiments did not show this effect in a multitude of adult samples with an overall heterogeneous SARS-CoV-2-specific T cell response. Nevertheless, SARS-CoV-2-specific CD8$^+$ T cell responses showed robust correlations across the AIM and optimized AIM+ICS assays, suggesting that while the sensitivity of the hybrid assay was impaired for AIM$^+$ CD8$^+$ T cell detection, its specificity was not (Fig. S4B). On the other hand, the hybrid AIM+ICS identified a higher magnitude (as well

as higher stimulation indices) of SARS-CoV-2-specific $CD4^+$ T cells in the study cohort compared to the AIM assay, suggesting that the diminished antibody concentrations were well-suited to the sensitive and specific analysis of AIM^+ $CD4^+$ T cells (Fig. 6A). Thus, while the hybrid AIM+ICS T cell panel designed here has the tremendous benefit of allowing the interrogation of multiple facets of SARS-CoV-2-specific T cell responses in children and adults, such as their phenotype, function, magnitude, and kinetics, it is apparent that the concurrent examination of multiple T cell markers and cytokines is not currently possible with a great degree of specificity as well as sensitivity for all the markers and T cell subsets involved. This preliminary analysis thus showed the suitability of the hybrid AIM+ICS for the detection of SARS-CoV-2-specific $CD4^+$ T cells from pediatric and adult samples of the study cohort, and suggested a greater need to rely on the paired cytokine data for the sensitive analysis of SARS-CoV-2-specific $CD8^+$ T cell responses.

While this study is well-suited to experimentally address numerous ongoing questions in the pediatric SARS-CoV-2 T cell field, here we have performed an initial analysis on a small subset of pediatric and adult donors. Interestingly, we observed a higher proportion of children mounting detectable SARS-CoV-2 (both Spike and non-Spike)-specific $CD4^+$ T cell responses compared to adults, with no significant differences between the frequencies of SARS-CoV-2-specific $CD4^+$ T cells across pediatric and adult groups, likely owing to a small sample size (Fig. 7). Whether this higher rate of SARS-CoV-2-specific $CD4^+$ T cell responses in children with mild or asymptomatic infection holds true upon analysis of a larger group of samples, and whether it is enabled upon primary infection by the larger naïve T cell repertoire of children remains to be seen. Additionally, while our preliminary analysis included well-balanced samples across pediatric and adult cohorts temporally spanning the entire disease course, the limited sample sets prevented the analysis of possibly differential kinetics of SARS-CoV-2-specific T cells across the two groups. Thus, it remains to be seen whether pediatric SARS-CoV-2-specific CD4+ T cells arise faster than the adult counterparts or differ in their durability. Interestingly, pediatric SARS-CoV-2-specific $CD4^+$ T cells appear to also be more functional, with a slightly higher fraction of antigen-responsive $CD4^+$ T cells (Spike and CD4 RE-specific) expressing GzmB, IFNg, IL-2, IL-10, IL-17 or TNFa upon restimulation (Fig. 8 and S7). Thus, while it is difficult to assess at this stage whether children's SARS-CoV-2-specific $CD4^+$ T cells are differentially polarized compared to their adult counterparts, it does appear that they are more capable of responding to their cognate SARS-CoV-2 antigen via cytokine secretion. Overall, should these findings hold in the larger study, it could mean that children benefit from a high frequency, high quality $CD4^+$ T cell immune response even in the absence of moderate or severe disease. Interestingly, only one study to date noted a higher magnitude of SARS-CoV-2-specific T cells (driven by Spike-specific, rather than non-Spike-specific T cell responses) in children with asymptomatic or mild infection, but could not discriminate between $CD4^+$ and $CD8^+$ T cell responses due to the experimental platform used; additionally, no data on the functionality of the SARS-CoV-2-specific T cells was presented (Dowell et al., 2022).

Even though the analysis of Ag-specific $CD8^+$ T cell responses was not optimal within the optimized hybrid AIM+ICS assay in terms of assay sensitivity (but not specificity), we nevertheless analyzed the differences emerging across the adult and pediatric groups in this preliminary study. Of note, while very few adults as well as children mounted discernible SARS-CoV-2-specific $CD8^+$ T cell responses, a smaller proportion of children mounted Spike and non-Spike-specific $CD8^+$ T cell responses when trends across all AIM marker pairs are considered. Overall, no clear trends emerged across all AIM marker pairs with regards to the frequency and stimulation indices of SARS-CoV-2-specific $CD8^+$ T cells in children compared to adults (Fig. S6). Additionally, given the low sensitivity of the hybrid AIM+ICS in identifying SARS-CoV-2 specific $CD8^+$ T cells, an alternative method of defining $CD8^+$ T cell responders might be helpful. Importantly, a point of contention in the field relates to whether children's immune responses are more focused on the Spike rather than the remainder of the SARS-CoV-2 proteome; in this regard, perhaps a more lenient way of defining CD8 responders in the present study, or an additional analysis of the magnitude of Spike- and non-Spike-specific $CD8^+$ T cell responses in responders alone will better contribute to that discussion. Additionally, given the

link between humoral immune responses and virus-specific $CD4^+$ T cell responses (Goldblatt et al., 2022; Sette & Crotty, 2022), an analysis of SARS-CoV-2 antibody responses in children and adults in the current study would help delineate whether potent antibody responses in children could contribute to viral control and thus offset the need for cytotoxic $CD8^+$ T cell responses. Overall, it is envisionable that even within the span of similar clinical disease presentation, different immunological mechanisms govern protective responses in children and adults. Opposingly, it is entirely within the realm of possibilities that a more potent initial innate or adaptive $CD4^+$ T cell response in children contributes to an earlier infection control, and thus less ongoing viral replication and bystander immune inflammation/activation are available to prime a potent, high-frequency $CD8^+$ T cell response. Importantly, SARS-CoV-2-specific $CD8^+$ T cells in children have rarely been assessed, given the preponderant use of techniques such as ELISpot which cannot differentiate between $CD4^+$ and $CD8^+$ T cell compartments. On the one hand, a study performed in children and adults with mild or asymptomatic SARS-CoV-2 infection found Spike-specific $CD8^+$ T cell responses of similar magnitude, but lower $CD8^+$ T cell responses against internal viral proteins in children (Rowntree et al., 2022). On the other hand, an earlier study noted a lower magnitude of $CD8^+$ T cells responsive to a peptide pool containing all SARS-CoV-2 structural proteins in children compared to adults following asymptomatic, mild or moderate infection; however, this study doesn't allow the discrimination of SARS-CoV-2-specific $CD8^+$ T cell antigenic specificity (Cohen et al., 2021). Nevertheless, more work is needed to verify the magnitude, quality and kinetics of SARS-CoV-2-specific $CD8^+$ T cell responses in children, and to unravel the cause-effect conundrum of possibly poorer $CD8^+$ T cell responses.

Given the low sensitivity of the hybrid AIM+ICS in assessing AIM^+ $CD8^+$ T cells, the characterization of the functional profile of Ag-responsive $CD8^+$ T cells becomes critical. The expression of $Cytokine^+$ within $CD8^+$ T cells showed similar or slightly higher levels of IFNg, IL-2, IL-10, IL-17, and TNFa following both Spike MP and CD4 RE MP stimulation, suggesting at least a similar functionality of the SARS-CoV-2-specific $CD8^+$ T cell response in children as in adults (Fig. S7). Of note, no study to date has assessed the functionality of SARS-CoV-2-specific $CD4^+$ and $CD8^+$ T cells using intracellular cytokine expression of a large array of cytokines, but rather relied on either $CD4^+$ or $CD8^+$ IFNg production alone, or cell culture supernatant analysis. In this regard, both methods exhibit a lower breadth and sensitivity compared to the hybrid AIM+ICS, and the latter technique cannot be used to identify the immune cell population responsible for secreting cytokines in response to restimulation. As such, more work will be needed to characterize the functionality as well as the possible functional polarization of Ag-specific $CD4^+$ and $CD8^+$ T cells in pediatric SARS-CoV-2 infection. In the context of this study, further analyses will be performed to map the degree of polyfunctionality in adult and pediatric SARS-CoV-2-specific $CD4^+$ and $CD8^+$ T cells, as well to characterize the immune subset composition of children and adults by analyzing the memory and T helper subset distribution in bulk as well as antigen-specific T cells.

With regards to the limitations of this study, here we have used a highly heterogeneous source of PBMCs for the hybrid AIM+ICS optimization experiments, such as vaccinated donors that received various doses of mRNA and/or viral vector COVID-19 vaccines as part of a previous study, convalescent donor PBMCs that were available in-house due to their very robust SARS-CoV-2-specific $CD4^+$ and/or $CD8^+$ T cell responses, as well as healthy donor PBMCs that were acquired via the Normal Blood Donor Program of the Institute and which were assumed to have a SARS-CoV-2-specific T cell response due to the mandatory vaccination policy of the Institute. To address this limitation, for each optimization experiment we included a balanced proportion of convalescent and vaccinated/ healthy donor PBMCs, so that the overall SARS-CoV-2-specific T cell response would encompass both strong and weak responses. An additional weakness with regards to the cell source used throughout optimization experiments was due to the use of fresh as well as refrozen PBMCs, depending on the in-house availability of previously mentioned categories. In this regard, given that the number of freeze-thaw cycles has an impact on AIM marker expression at baseline, different experiments might show different DMSO background levels depending on the source and condition of cells

used. Ultimately, the inclusion of heterogenous SARS-CoV-2-specific T cell responses in the optimization experiments could also be perceived as an advantage, given that it enabled us to finetune the assay in preparation for a wide range of possible T cell responses of the pediatric study cohort, and the applicability of this assay to other study cohorts as well. Lastly, given the limited sample set which was included in the preliminary analysis of the study cohort, reaching statistical power was not feasible. The analysis of the entire study cohort will enable the assessment of SARS-CoV-2 specific T cell kinetics in children and adults, as well as the analysis of the impact of age on the properties of pediatric SARS-CoV-2-specific T cell responses in children. Nevertheless, here we show as proof of principle the use of the hybrid AIM+ICS assay for the characterization of pediatric SARS-CoV-2-specific $CD4^+$ and $CD8^+$ T cells that will provide the most comprehensive dataset currently available in the field.

While the research disparity in the pediatric relative to the general population is partly due to the relative difficulty of obtaining children's samples, several reasons prompt a renewed effort in this direction. Of note, the hybrid AIM+ICS panel designed here could help maximize the insights gained from limited pediatric samples. Most importantly, the current view that children are at lower risk of severe COVID-19 inherently prompts a more careful examination of the factors contributing to protective immunity, and especially to their durability. Given the emerging understanding of the crucial role that T cells play in protection against SARS-CoV-2, more work is needed to assess the ways in which SARS-CoV-2-specific T cell responses mounted by children of various ages across the entire disease spectrum differ from those analyzed in adult populations to date. The present study will thereby contribute to a better understanding of the development of SARS-CoV-2-specific $CD4^+$ and $CD8^+$ T cell responses in children with mild and asymptomatic infection, which in the end constitute the likeliest outcome of SARS-CoV-2 infection in children. Furthermore, the in-depth knowledge of the development, maintenance, and durability of SARS-CoV-2-specific T cell responses in children will shed light on the level of T cell-mediated protection afforded by asymptomatic or mild SARS-CoV-2 infection, and will thus help inform on the true need for vaccine uptake and antiviral treatments following (re)-infection in the general pediatric population. Thus, this study will serve as a steppingstone towards a more comprehensive understanding of children's cellular immunity against SARS-CoV-2, with possible implications for age-personalized vaccine design and treatment. Ultimately, this study will help further our general knowledge of pediatric adaptive immune responses following a primary respiratory viral infection at a single-cell level across the entire time course of infection, which is an important knowledge gap in the field.

Methods

Study design

The aim of this study was to characterize the frequency, phenotype, function, and kinetics of SARS-CoV-2 specific $CD4^+$ and $CD8^+$ T cells in children aged 0-20 years following mild or asymptomatic SARS-CoV-2 infection.

Study cohort

132 children were recruited by Dr. Matthew Kelly's group at the Duke University Hospital System (the BRAVE cohort). 24 children (18.2%) had asymptomatic SARS-CoV-2 infection, 93 (70.5%) had mildly symptomatic SARS-CoV-2 infection, whereas 15 (11.4%) did not develop SARS-CoV-2 infection. Children were grouped in the following ages: 0-4 years (n=30, median age 3.1), 5-11 years (n=36, median age 7.8), 12-15 years (n=31, median age 13.8), and 16-20 years (n=35, median age 17.9). All children with mild or asymptomatic SARS-COV-2 infection were PCR-positive (n=117, 88.6%), whereas PCR-negative children served as healthy age-matched controls (n=15, 11.4%). PCR-negative children were identified following a positive diagnosis in their immediate family. A total of 198 peripheral blood samples were obtained, including longitudinal samples where available. Samples were collected in the period April 2020 – June 2021, which preceded the vaccination of children in the US. Samples were further divided into the acute phase of infection (collected at 0-14 days post-PCR positivity, n=80), or convalescent phase (collected at >14 days post-PCR positivity, n=118). Additionally, 55 unvaccinated adults (median age 42.4) were recruited, of which 47 (85.5%) developed mild symptomatic COVID-19, and 8 (14.5%) did not become SARS-CoV-2 PCR-positive nor developed COVID-19. A total of 100 samples were obtained, including longitudinal samples where available. Samples were collected in the period April 2020 – June 2021. Samples were further divided into the acute phase of infection (collected at 0-14 days post-symptom onset, n=30), or convalescent phase (collected at >14 days post-symptom onset, n=62). The demographic and clinical features of the study cohort are detailed in Table 2.

For the preliminary analysis of SARS-CoV-2-specific $CD4^+$ and $CD8^+$ T cell responses, we included a heterogeneous subset of the study cohort described above. 19 donors were included, with a total of 30 samples including multiple longitudinal timepoints where available. The distribution of samples across groups in terms of longitudinal samples available per donor, donor age, and timing post-infection are represented visually in Figure S5. Briefly, we included 18 pediatric and 12 adult samples, of which 2 and 2 respectively were uninfected age-matched controls. 3 longitudinal samples were available from 1 adult and 1 child, 2 longitudinal samples were available from 3 adults and 5 children, and the remainder of donors provided only 1 sample. The ages of children ranged between 0.57 and 19.49 years, with a median age of 12.69; the ages of adults ranged between 28.6 and 52.1 years, with a median age of 33.9. The days post-symptom onset ranged between 5 and 193 days in children (median 64 days), whereas in adults it ranged between 6 and 188 (median 61 days).

Table 2: Demographics and clinical features of the study cohort.

	0-4 years (n=30)	5-11 years (n=36)	12-15 years (n=31)	16-20 years (n=35)	Total children (n=132)	Total adults (n=55)
Median age, years	3.1	7.8	13.8	17.9	11.8	42.4
Sex (%)						
Female	13 (43.3%)	14 (38.9%)	18 (58.1%)	17 (48.6%)	62 (47.0%)	27 (49.1%)
Male	17 (56.7%)	22 (61.1%)	13 (41.9%)	18 (51.4%)	70 (53.0%)	28 (50.9%)

Illness severity (%)						
Asymptomatic	3 (10.0%)	10 (27.8%)	5 (16.1%)	6 (17.1%)	24 (18.2%)	0 (0.0%)
Mild symptomatic	23 (76.7%)	23 (63.9%)	23 (74.2%)	24 (68.6%)	93 (70.5%)	47 (85.5%)
COVID-19 negative	4 (13.3%)	3 (8.3%)	3 (9.7%)	5 (14.3%)	15 (11.4%)	8 (14.5%)
SARS-CoV-2 PCR (%)						
positive	26 (86.7%)	33 (91.7%)	28 (90.3%)	30 (85.7%)	117 (88.6%)	47 (85.5%)
negative	4 (13.3%)	3 (8.3%)	3 (9.7%)	5 (14.3%)	15 (11.4%)	8 (14.5%)
Viral load (copies/uL), mean	1557253	24911497.72	19870404.89	1590268.886	11811396.41	26960430.35
PBMC samples						
acute (<14 days)	20	20	20	20	80	30
convalescent (>14 days)	14	30	26	28	98	62
COVID-19 negative	5	3	4	8	20	8
Sample collection dates	May 2020 - May 2021	May 2020 - June 2021	April 2020 - June 2021	May 2020 - May 2021	April 2020 - June 2021	April 2020 - June 2021
Sample collection: days post-diagnosis, mean (range)	48.7 (0-183)	73.1 (-2-186)	66.8 (-2-191)	74.2 (0-189)	67.1 (-2-191)	N/A
Sample collection: days post-symptom onset, mean (range)	49.4 (-1-190)	63.2 (0-190)	69.5 (-1-191)	79.4 (4-194)	66.3 (-1-194)	71.1 (0-211)
Race-ethnicity (%)						
White - not Hispanic or Latino	4 (13.3%)	3 (8.3%)	6 (19.4%)	5 (14.3%)	18 (13.6%)	33 (60.0%)
Hispanic or Latino	18 (60.0%)	25 (69.4%)	18 (58.1%)	27 (77.1%)	88 (66.7%)	1 (1.8%)
Asian	1 (3.3%)	0 (0.0%)	0 (0.0%)	0 (0.0%)	1 (0.8%)	3 (5.5%)
American Indian/ Alaska Native	0 (0.0%)	0 (0.0%)	0 (0.0%)	0 (0.0%)	0 (0.0%)	2 (3.6%)
Black or African American	4 (13.3%)	5 (13.9%)	4 (12.9%)	1 (2.9%)	14 (10.6%)	11 (20.0%)
Native Hawaiian- Pacific Islander	0 (0.0%)	0 (0.0%)	0 (0.0%)	0 (0.0%)	0 (0.0%)	1 (1.8%)
>1 race	2 (6.7%)	3 (8.3%)	3 (9.7%)	2 (5.7%)	10 (7.6%)	1 (1.8%)
Other/unknown	1 (3.3%)	0 (0.0%)	0 (0.0%)	0 (0.0%)	1 (0.8%)	3 (5.5%)

Human samples

For optimization experiments, a mix of COVID-19 convalescent and vaccinated/healthy donor PBMCs were used. Healthy donor PBMCs (assumed to have received 2-3 doses of an FDA-approved COVID-19

vaccine due to the Institute's COVID-19 mandatory vaccination policy) were obtained following written informed consent from the La Jolla Institute for Immunology Normal Blood Donor Program (VD-057). Refrozen PBMCs remaining from donors enrolled in the Heterologous Vaccine Study were used; these donors received either one dose of the Oxford/AstraZeneca vaccine ChAdOx1-S and one dose of an FDA-approved mRNA vaccine, or two homologous doses of either vaccine; note that different sample draw dates post-vaccination were included. COVID-19 convalescent samples were obtained either from the San Diego Blood Bank or from BioIVT following written informed consent. Samples were stored in a liquid nitrogen tank. A subset of human samples was freeze-thawed multiple times and used in subsequent experiments.

Activation-Induced Marker (AIM) assay

Cryopreserved peripheral blood mononuclear cells (PBMCs) were thawed in pre-warmed AIM medium (RPMI 1640 1X [Corning 10-041-CV] supplemented with 1% Penicillin-Streptomycin [Gibco, 15140-122], 1% GlutaMAX [Gibco, 35050061], and 5% human serum AB [GeminiBio, 100-512]) with 1:5000 benzonase nuclease 25KU (EMD Millipore Corp, 71206-25KUN), and resuspended in pre-warmed AIM medium. Cells were rested for 1 hour at 37°C, 5% CO_2, and counted using the Muse Count & Viability kit (Luminex, MCH600103) using the Guava Muse (Luminex). PBMCs were resuspended at a concentration of $10x10^6$ cells/ml and plated in a U-bottom 96-well plate (Sarstedt, 82.1582001) at $1x10^6$ cells/well. Cells were incubated with the following mix of chemokine receptor antibodies: CXCR5 AF700 (1:200; BioLegend, 356915), CXCR3 BV605 (1:200, BioLegend, 353728) CCR7 BV711 (1:100, BioLegend, 353228) and CCR6 BUV496 (1:200, BD Horizon, 612948), and anti-CD40 blocking antibody (1:200, Miltenyi Biotec, 130-094-133) for 15 min at 37°C, 5% CO_2. Without washing, cells were then stimulated with SARS-CoV-2 peptide megapools (MPs, 1 mg/ml) at a final concentration of 1 ug/ml per peptide, reaching a final volume of 200 uL/well. Two SARS-CoV-2 MPs were used for *ex vivo* stimulation: a SARS-CoV-2 spike MP containing 253 overlapping 15-mer peptides spanning the entire spike protein, allowing the Ag-specific stimulation of both $CD4^+$ and $CD8^+$ T cells (Grifoni et al., 2020), and a peptide MP spanning the non-spike proteome of SARS-CoV-2, containing MHC class II, experimentally-defined epitopes (hereon referred to as CD4 remainder megapool, or CD4 RE) (Grifoni et al., 2021). Negative control wells were stimulated with an equimolar amount of DMSO, and positive control wells were stimulated with SEB (1 mg/ml, Toxin Technology) at a final concentration of 1 ug/ml. Cells were incubated for 22-24 hours at 37°C, 5% CO_2. Stimulated cells were washed in phosphate buffered saline (PBS, Corning, 21-040-CV) and resuspended in 50 uL FACS buffer (PBS with 3% FBS, [GeminiBio, 900-108]) with 10% Fc Receptor Blocking solution (BioLegend, 422302) for 15 min at room temperature (RT). Cells were then washed in PBS and stained with CD3 BUV395 (1:200, BD Horizon, 563546), ICOS BUV563 (1:50, BD OptiBuild, 741421), CD38 BUV661 (1:100, BD Horizon, 612969), PD-1 BUV737 (1:100, BD Horizon, 612791), CD8 BUV805 (1:800, BD Horizon, 612889), 4-1BB BV421 (1:50, BioLegend, 309820), CD14 BV510 (1:100, BioLegend, 367124), CD16 BV510 (1:200, BioLegend, 302048), CD20 BV510 (1:50, BioLegend, 302340), CD45RA BV570 (1:400, BioLegend, 304132), CD27 BV785 (1:100, BioLegend, 302832), CD69 AF488 or FITC (1:100, BioLegend 310916 or 310904 respectively), CD4 PerCP-eF710 or APC-Fire810 (1:50, Invitrogen, 46-0047-42, or BioLegend, 344661 respectively), CD40L PE-Dazzle594 (1:100, BioLegend, 310840), OX-40 AF647 or APC (1:50, BioLegend, 350018 or 350008 respectively), and Fixable Viability Dye eFluor 780 (1:2000, eBioscience, 65-0865-14) in FACS buffer with 1:5 Brilliant Stain Buffer Plus (BD Biosciences, 566385) for 30 min at 4°C. Cells were then washed and resuspended in FACS buffer prior to acquisition on a 5-laser Cytek Aurora (Cytek Biosciences) using SpectroFlo (Cytek Biosciences, versions 2.2.0.4 and 3.0.3). Data analysis was performed in FlowJo software v10 (Tree Star).

Hybrid Activation-Induced Marker and Intracellular Cytokine Stain (AIM + ICS) assay

The *ex vivo* PBMC stimulation was performed as described for the AIM assay. Following 22-24 hours of incubation, cells were stained (without washing) for 4 hours at 37°C, 5% CO_2, with an intracellular transport blocking and antibody mix containing the following: BD GolgiStop (1:200, BD Biosciences, 51-

2092KZ), BD GolgiPlug (1:200, BD Biosciences, 51-2301KZ), ICOS BUV563 (1:150, BD OptiBuild, 741421), PD-1 BUV737 (1:200, BD Horizon, 612791), 4-1BB BV421 (1:200, BioLegend, 309820), CD69 FITC (1:100 unless otherwise specified, BioLegend, 310904), CD40L PE-Dazzle594 (1:200 unless otherwise specified, BioLegend, 310840), and OX-40 APC (1:100, BioLegend, 350008). Alternatively, to allow for optimal cytokine secretion and gating of Cytokine$^+$ AIM$^+$ T cells, 1 well per donor (where applicable) was stimulated with 0.05 ug/ml PMA (Sigma-Aldrich, P1585-1MG) and 0.25 ug/ml ionomycin (Sigma-Aldrich, I0634-5MG) together with the intracellular transport blocking and antibody mix, and incubated for 4 hours at 37°C, 5% CO_2. The cells were then washed in PBS and resuspended in 50uL FACS buffer with 10% Fc Receptor Blocking solution (BioLegend, 422302) for 15 min at RT. Cells were then washed in PBS and surface stained with CD3 BUV395 (1:200, BD Horizon, 563546), CD38 BUV661 (1:100, BD Horizon, 612969), CD8 BUV805 (1:800, BD Horizon, 612889), CD14 BV510 (1:100, BioLegend, 367124), CD16 BV510 (1:200, BioLegend, 302048), CD20 BV510 (1:50, BioLegend, 302340), CD45RA BV570 (1:400, BioLegend, 304132), CD27 BV785 (1:100, BioLegend, 302832), CD4 PerCP-eF710 or APC-Fire810 (1:50, Invitrogen, 46-0047-42, or BioLegend, 344661 respectively), and Fixable Viability Dye eFluor 780 (1:2000, eBioscience, 65-0865-14) in FACS buffer with 20% Brilliant Stain Buffer Plus (BD Biosciences, 566385) for 30 min at 4°C. Cells were then washed twice in FACS buffer and resuspended in 4% formaldehyde (10% formaldehyde [Polysciences, 04018-1] in PBS) for 10 min at 4°C. Cells were washed three times in permeabilization buffer (0.5% w/v saponin [Sigma-Aldrich, 47036-50G-F], 10% BSA and 1% sodium azide in PBS) and resuspended for 5 min at RT in blocking buffer (10% human serum AB in permeabilization buffer). Without washing, cells were stained intracellularly with the following antibodies: TNFalpha eF450 (1:50, EBioscience, 48-7349-42), IL-2 BV650 (1:50, BioLegend, 500334), IL-17A BV750 (1:50, BD Horizon, 566358), Granzyme B AF532 (1:50, EBioscience, 58-8896-42), IL-10 BB700 (1:50, BD Horizon, 566568), and IFNg PE-Cy7 (1:600, EBioscience, 25-7319-82) in permeabilization buffer with 20% Brilliant Stain Buffer Plus (BD Biosciences, 566385) for 30 min at 4°C. Cells were then washed once in permeabilization buffer and once in FACS buffer, and resuspended in FACS buffer prior to acquisition on a 5-laser Cytek Aurora (Cytek Biosciences) using SpectroFlo (Cytek Biosciences, versions 2.2.0.4 and 3.0.3). Data analysis was performed in FlowJo software v10 (TreeStar).

Data Analysis and Statistics

Data analysis was carried out in FlowJo software v10 (TreeStar). Statistical analyses and data plotting were performed in GraphPad Prism software 9.4.0. Frequencies of Ag-specific T cell responses were calculated as frequency of AIM$^+$ cells in the respective stimulation condition minus the frequency of AIM$^+$ cells in the negative control (DMSO) per donor. The stimulation indices of Ag-specific T cells were calculated as the ratio of the magnitude of the AIM$^+$ T cell response divided by the magnitude of the background in the DMSO condition. T cell responses described as frequencies were plotted on a logarithmic scale, and geometric means were used to summarize the data. Stimulation indices were plotted on a linear scale, or on a logarithmic scale where necessary, and medians were used to summarize the data. Paired data were analyzed using Wilcoxon-matched pairs signed rank tests, whereas unpaired data were analyzed using Mann-Whitney U tests. Background-subtracted AIM$^+$ or Cytokine$^+$ AIM$^+$ frequencies equal to or smaller than 0 were set to 0.001% for CD4$^+$ T cells and 0.0001% for CD8$^+$ T cells to allow plotting on a logarithmic axis; this was shown where applicable as the limit of detection.

Table 3: Overview of reagents and resources used in the study.

REAGENT OR RESOURCE	SOURCE	IDENTIFIER
AIM and AIM+ICS assays		
Corning RPMI 1640 1X with L-Glutamine & 25mM HEPES	Corning	10-041-CV
Penicillin-Streptomycin (10,000 U/mL)	Gibco, ThermoFisher Scientific	15140-122
GlutaMAX Supplement	Gibco, ThermoFisher Scientific	35050061
Benzonase Nuclease HC, Purity >99%	EMD Millipore Corp	71206-25KUN
GemCell Human serum AB	GeminiBio	100-512

Muse Count & Viability kit	Luminex	MCH600103
Spike megapool	(Grifoni et al., 2020)	
CD4 RE megapool	(Grifoni et al., 2021)	
DMSO	Sigma-Aldrich	D2650-5X10ML
SEB	Toxin Technology	BT202
Phorbol 12-myristate 13-acetate (PMA)	Sigma-Aldrich	P1585-1MG
Ionomycin calcium salt from Streptomyces conglobatus	Sigma-Aldrich	I0634-5MG
Corning Phosphate-Buffered Saline, 1X without calcium and magnesium	Corning	21-040-CV
Foundation Fetal Bovine Serum	GeminiBio	900-108
BD GolgiStop (Protein Transport Inhibitor containing Monensin)	BD Biosciences	554724, 51-2092KZ
BD GolgiPlug (Protein Transport Inhibitor containing Brefeldin A)	BD Biosciences	555029, 51-2301KZ
Formaldehyde (Methanol Free), 10% UltraPure EM Grade	Polysciences	04018-1
Saponin	Sigma-Aldrich	47036-50G-F
Bovine Serum Albumin	Sigma-Aldrich	D2650-5X10ML
Sodium Azide		
CD40 Antibody, anti-human, pure-functional grade (HB14)	Miltenyi Biotec	130-094-133
Human TruStain FcX (Fc Receptor Blocking Solution)	BioLegend	422302
Brilliant Stain Buffer Plus	BD Horizon, BD Biosciences	566385
Round bottom 96-well plate	Sarstedt	82.1582.001
PBMCs	LJI Blood Donor Program San Diego Blood Bank BioIVT Heterologous Vaccine Study	
Antibodies		
CXCR5 [CD185] AF700 (J252D4)	BioLegend	356915
CXCR3 [CD183] BV605 (G025H7)	BioLegend	353728
CCR7 [CD197] BV711 (G043H7)	BioLegend	353228
CCR6 [CD196] BUV496 (11A9)	BD Horizon	612948
CD3 BUV395 (UCHT1)	BD Horizon	563546
CD38 BUV661 (HIT2)	BD Horizon	612969
CD8 BUV805 (SK1)	BD Horizon	612889
CD14 BV510 (63D3)	BioLegend	367124
CD16 BV510 (3G8)	BioLegend	302048
CD20 BV510 (2H7)	BioLegend	302340
CD45RA BV570 (HI100)	BioLegend	304132
CD27 BV785 (O323)	BioLegend	302832
CD4 PerCPeF710 (SK3)	Invitrogen	46-0047-42
CD4 APC-Fire810 (SK3)	BioLegend	344661
Fixable Viability Dye eFluor 780	eBioscience	65-0865-14
ICOS [CD278] BUV563 (DX29)	BD OptiBuild	741421
PD-1 [CD279] BUV737 (EH12.1)	BD Horizon	612791
4-1BB [CD137] BV421 (4B4-1)	BioLegend	309820
CD69 FITC (FN50)	BioLegend	310904
CD69 AF488 (FN50)	BioLegend	310916
CD40L [CD154] PE-Dazzle594 (24-31)	BioLegend	310840
OX-40 [CD134] APC (Ber-ACT35)	BioLegend	350008
OX-40 [CD134] AF647 (Ber-ACT35)	BioLegend	350018
TNF alpha eF450 (MAb11)	eBioscience, Invitrogen	48-7349-42
IL-2 BV650 (MQ1-17H12)	BioLegend	500334
IL-17A BV750 (N49-653)	BD Horizon	566358
IL-10 BB700 (JES3-19F1)	BD Horizon	566568
Granzyme B AF532 (N4TL33)	eBioscience, Invitrogen	58-8896-42
IFNg PE-Cy7 (4S.B3)	eBioscience, Invitrogen	25-7319-82

Software		
FlowJo v10	TreeStar Inc.	
GraphPad Prism 9.4.0	GraphPad Software, LLC.	
SpectroFlo	Cytek BioSciences	
Instruments		
Guava Muse Cell Analyzer	Luminex	
Cytek Aurora	Cytek BioSciences	

Supplementary information

	BUV395	BUV496	BUV563	BUV661	BUV737	BUV805	BV421	eFluor 450	BV510	BV570	BV605	BV650	BV711	BV750	BV785	FITC	Alexa Fluor 532	BB700	PE-Dazzle594	PE-Cy7	APC	Alexa Fluor 700	eFluor 780	APC-Fire 810
BUV395	1																							
BUV496	0.25	1																						
BUV563	0.05	0.29	1																					
BUV661	0.04	0.02	0.06	1																				
BUV737	0.03	0.01	0.01	0.37	1																			
BUV805	0.11	0.03	0.01	0.1	0.39	1																		
BV421	0.05	0.09	0.01	0	0	0.01	1																	
eFluor 450	0	0.08	0	0	0	0	0.85	1																
BV510	0.02	0.48	0.22	0.04	0.02	0	0.17	0.27	1															
BV570	0.01	0.09	0.37	0.06	0.02	0	0.15	0.14	0.54	1														
BV605	0.01	0.05	0.2	0.17	0.05	0.01	0.06	0.06	0.4	0.7	1													
BV650	0	0.02	0.04	0.4	0.13	0.02	0.09	0.08	0.16	0.25	0.53	1												
BV711	0	0	0.01	0.25	0.41	0.09	0.09	0.08	0.06	0.07	0.17	0.45	1											
BV750	0	0	0	0.09	0.37	0.14	0.05	0.04	0.04	0.04	0.1	0.23	0.69	1										
BV785	0	0	0	0.05	0.25	0.21	0.07	0.07	0.03	0.03	0.07	0.15	0.49	0.82	1									
FITC	0.01	0.09	0.06	0	0	0	0.01	0.01	0.06	0.03	0.01	0	0	0	0	1								
Alexa Fluor 532	0.03	0.02	0.25	0	0	0	0.02	0.02	0.02	0.08	0.04	0.01	0	0	0	0.55	1							
BB700	0	0	0.02	0.33	0.3	0.05	0	0	0.05	0.08	0.16	0.37	0.53	0.3	0.21	0.02	0.07	1						
PE-Dazzle594	0.01	0.02	0.36	0.13	0.02	0	0	0	0.09	0.41	0.47	0.16	0.04	0.01	0.01	0.06	0.3	0.18	1					
PE-Cy7	0	0	0.01	0.05	0.14	0.08	0	0	0	0.01	0.03	0.04	0.11	0.15	0.17	0	0.01	0.17	0.05	1				
APC	0	0	0.03	0.78	0.24	0.02	0	0	0.02	0.05	0.14	0.37	0.23	0.07	0.04	0	0	0.33	0.16	0.05	1			
Alexa Fluor 700	0	0.01	0	0.42	0.51	0.05	0	0	0.01	0	0.03	0.16	0.44	0.17	0.1	0	0	0.38	0.03	0.09	0.49	1		
eFluor 780	0	0	0	0.12	0.33	0.24	0	0	0.01	0.01	0.02	0.06	0.22	0.25	0.32	0	0	0.16	0.01	0.2	0.14	0.33	1	
APC-Fire 810	0	0	0	0.1	0.21	0.24	0	0	0	0	0.01	0.05	0.12	0.12	0.18	0	0	0.1	0.01	0.2	0.13	0.22	0.73	1

Figure S1: Similarity indices of the fluorophores included in the 24-color spectral flow cytometry T cell panel. *Figure was generated using the Cytek Full Spectrum viewer software (https://spectrum.cytekbio.com/).*

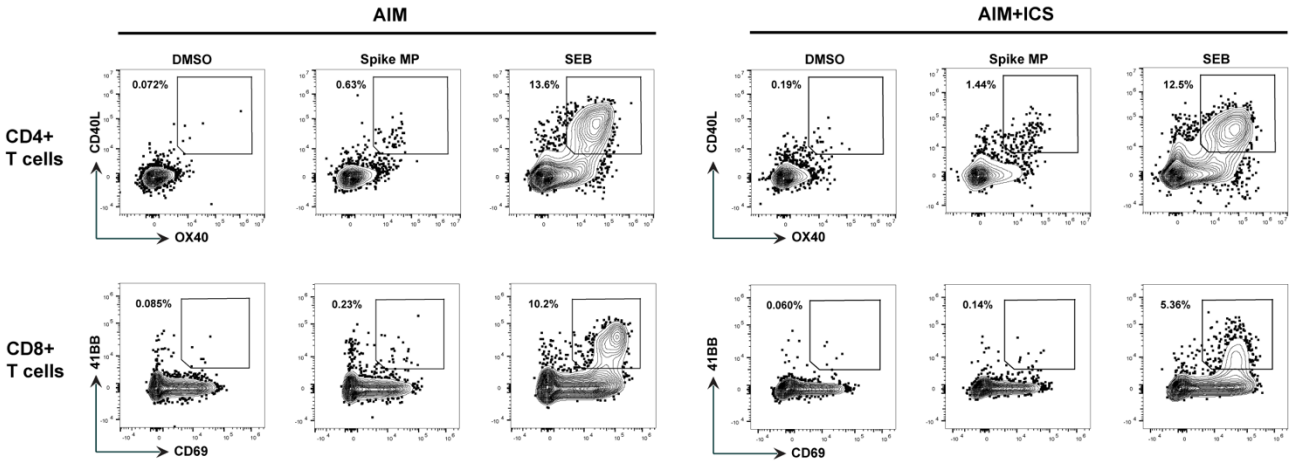

Figure S2**: **Representative flow cytometry plots showing the head-to-head comparison of AIM and AIM+ICS assays. One significant AIM marker pair is shown for each T cell subset: OX40$^+$ CD40L$^+$ cells for the CD4$^+$ T cell compartment, and CD69$^+$ 41BB$^+$ cells for the CD8$^+$ T cell compartment. The same COVID-19 convalescent control is shown for both AIM (**left**) and AIM+ICS assays (**right**).

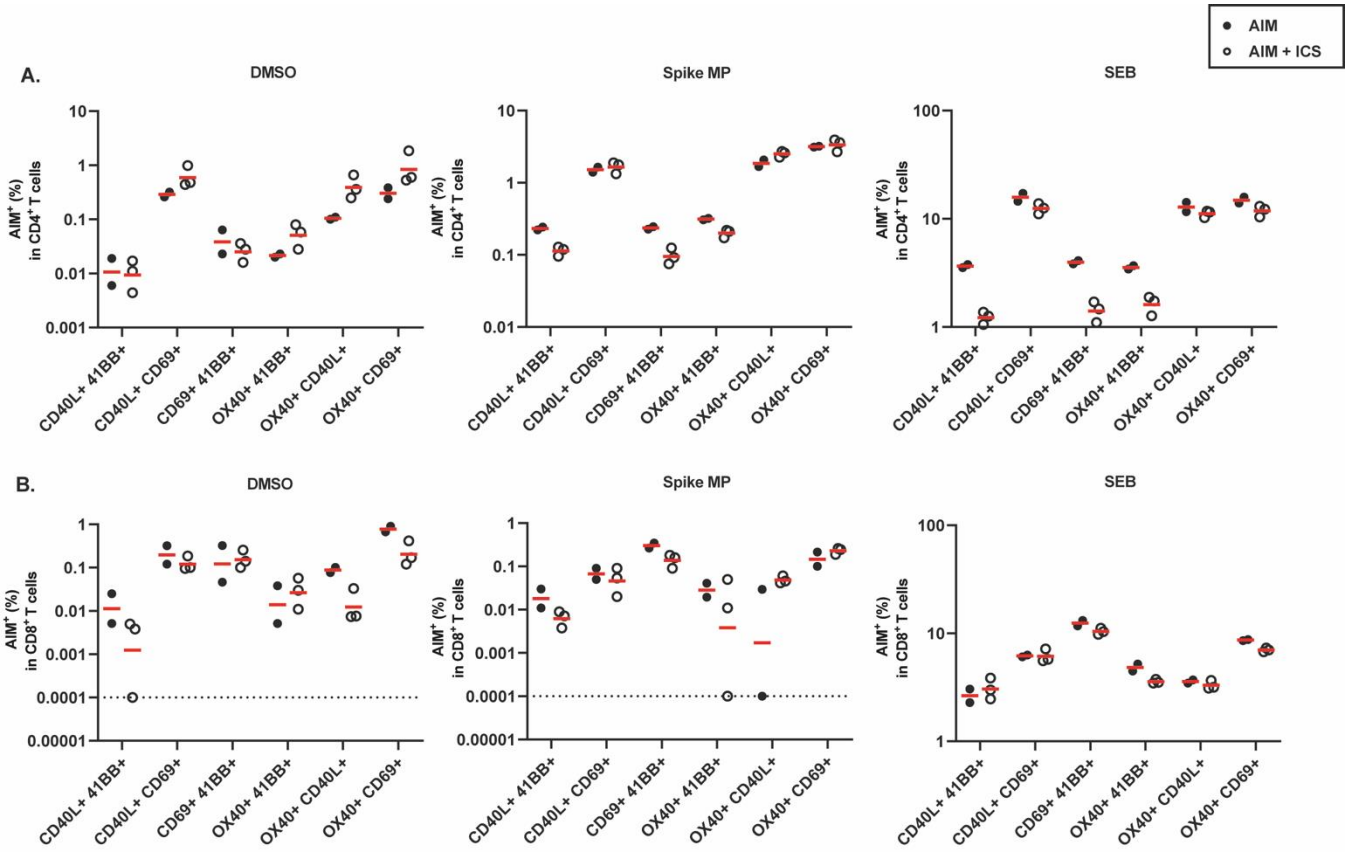

Figure S3: **Reliability of AIM or AIM+ICS assays** in detecting Ag-specific CD4$^+$ (**A**) and CD8$^+$ T cells (**B**) across n=2 (AIM) or n=3 (AIM+ICS) independent experiments across 3 stimulation conditions. Dotted line indicates limit of detection. The same COVID-19 convalescent control is shown in (A) and (B).

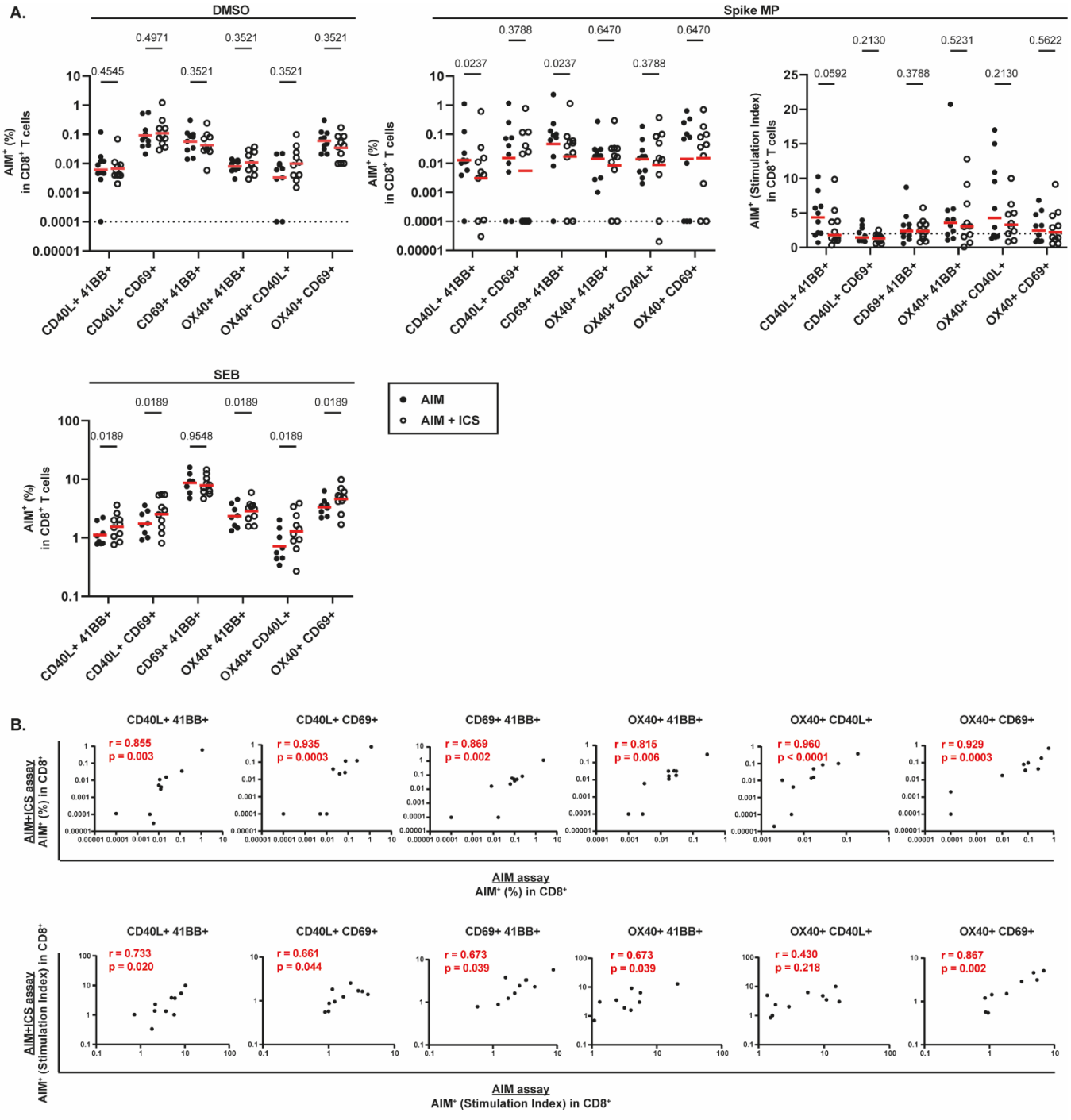

Figure S4: Head-to-head comparison of AIM and optimized hybrid AIM+ICS assays in adult and pediatric samples within the CD8⁺ T cell compartment (relates to Fig. 6). **A:** Frequency and stimulation indices of AIM⁺ CD8⁺ T cells following DMSO (**top left**), Spike MP (**top middle** and **right**, respectively), or SEB stimulation (**bottom**) in either AIM or AIM+ICS assays. Wilcoxon matched-pairs ranked sign test, with two-stage linear step-up procedure of Benjamini, Krieger and Yekutieli. **B:** Frequency (**top**) and stimulation indices (**bottom**) of AIM⁺ CD8⁺ T cells following Spike MP stimulation displayed as correlations between AIM and AIM+ICS assays across AIM marker pairs. Correlation coefficients and P-values are shown following non-parametric Spearmen correlation analysis. N=10; paired data; 4 adult COVID-19 convalescent, 2 adult vaccinated, and 4 pediatric infected donors.

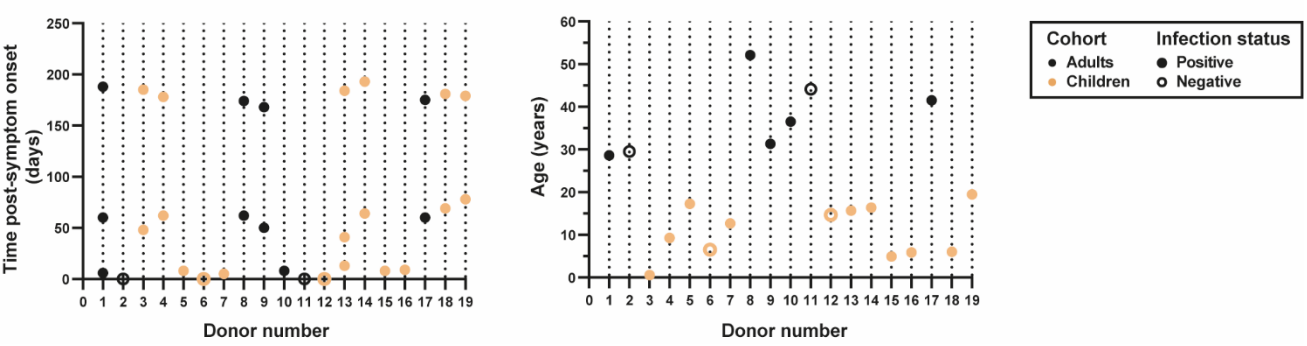

Figure S5: Description of adult and pediatric samples included in the preliminary study, including number and timing post-infection of longitudinal (paired) samples per donor, infection status, and age of donors. Black denotes adult samples, orange denotes children samples; full circles denote SARS-CoV-2 PCR-positive donors, empty circles indicate SARS-CoV-2 PCR-negative donors.

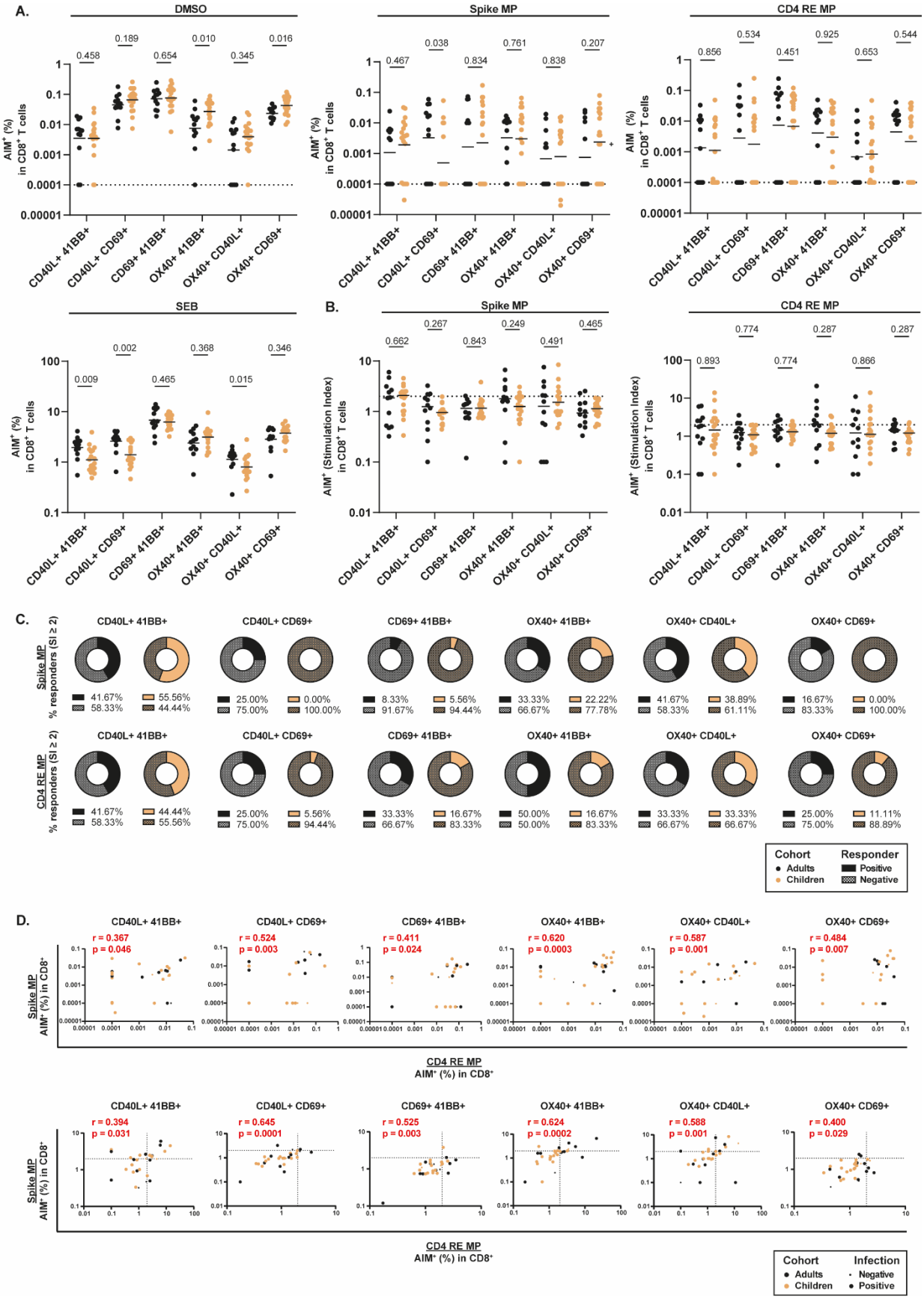

Figure S6: Preliminary analysis of SARS-CoV-2-specific CD8⁺ T cell responses in 9 adults and 10 children; relates to Figure 7. **A:** Frequency of AIM⁺ CD8⁺ T cells following DMSO (**top left**), Spike MP (**top middle**), CD4 RE MP (**top right**), or SEB stimulation (**bottom**). Mann-Whitney test; dotted line indicates the limit of detection. **B:** Stimulation indices of AIM⁺ CD8⁺ T cells following Spike

MP (**left**) or CD4 RE MP stimulation (**right**) across AIM marker pairs. Dotted line indicates the threshold of positivity, where responses equal to or greater than 2 are considered positive (i.e. SARS-CoV-2 responder). Mann-Whitney test. **C:** Pie charts showing the frequency of SARS-CoV-2 responders (defined as Stimulation index ≥2) to Spike MP (**top**) and CD4 RE MP (**bottom**) between adult and children cohorts. **D:** Frequency (**top**) and stimulation indices (**bottom**) of AIM$^+$ CD8$^+$ T cells displayed as correlations between Spike MP and CD4 RE MP-specific T cell responses. Correlation coefficients and P-values were calculated using non-parametric Spearmen correlation analysis. Adults are shown in black, and children are shown in orange; infection status is denoted by the relative size of the sample. N=30; unpaired data; 10 infected and 2 uninfected (SARS-CoV-2 PCR-negative) adult samples, 16 infected and 2 uninfected (SARS-CoV-2 PCR-negative) children samples. SI: Stimulation Index.

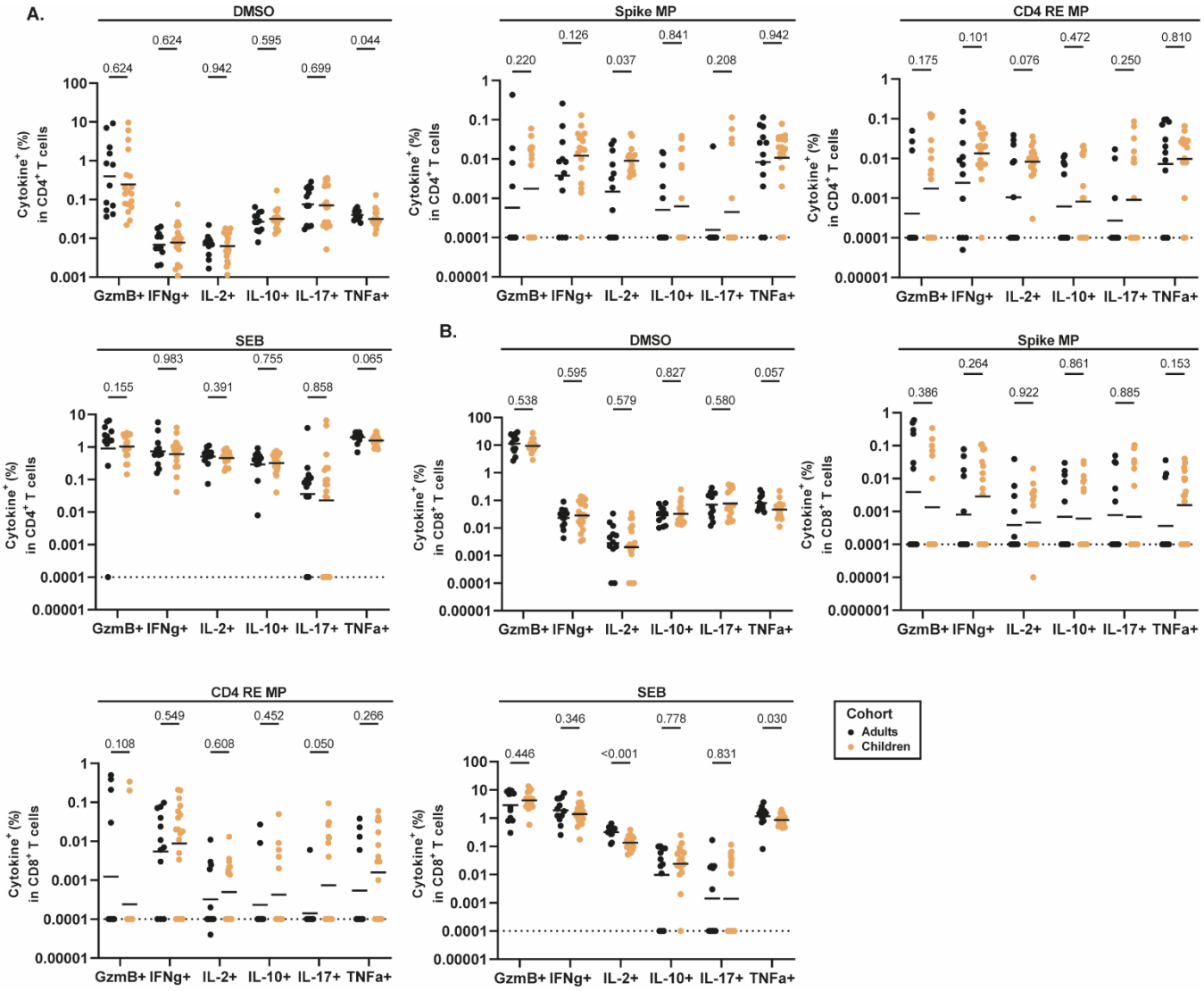

Figure S7: Preliminary analysis of cytokine expression by SARS-CoV-2-specific CD4$^+$ and CD8$^+$ T cells in 9 adults and 10 children, relates to Figure 8. **A:** Frequency of Cytokine$^+$ CD4$^+$ T cells following DMSO (**top left**), Spike MP (**top middle**), CD4 RE MP (**top right**), or SEB stimulation (**bottom**). Mann-Whitney test; dotted line indicates the limit of detection. **B:** Frequency of Cytokine$^+$ CD8$^+$ T cells following DMSO (**top middle**), Spike MP (**top right**), CD4 RE MP (**bottom left**), or SEB stimulation (**bottom middle**). Mann-Whitney test; dotted line indicates the limit of detection. N=30; unpaired data; 10 infected and 2 uninfected (SARS-CoV-2 PCR-negative) adult samples, 16 infected and 2 uninfected (SARS-CoV-2 PCR-negative) children samples.

Acknowledgements

I would like to thank prof. Shane Crotty for the incredible opportunity of performing my final master's internship in his lab. Equally, I would like to extend my thanks to Dr. Numana Bhat for her guidance during my project, for the trust she placed in me as well as for the very interesting scientific discussions. I would also like to thank Amber Myers for her continued support in the lab. Lastly, I am grateful to Dr. Tasha Altheide and Paul Lopez for helpful feedback on this manuscript, as well as to all Crotty Lab members for helpful input throughout my project.

Works cited

Amodio, D., Cotugno, N., & Palma, P. (2022). COVID-19 in children: From afterthought to unknown. In *Cell Reports Medicine* (Vol. 3, Issue 3). Cell Press. https://doi.org/10.1016/j.xcrm.2022.100558

Brodin, P. (2022). SARS-CoV-2 infections in children: Understanding diverse outcomes. In *Immunity* (Vol. 55, Issue 2, pp. 201–209). Cell Press. https://doi.org/10.1016/j.immuni.2022.01.014

Brummelman, J., Pilipow, K., & Lugli, E. (2018). The Single-Cell Phenotypic Identity of Human CD8 + and CD4 + T Cells. In *International Review of Cell and Molecular Biology* (Vol. 341). Elsevier Ltd. https://doi.org/10.1016/bs.ircmb.2018.05.007

Bundle, N., Dave, N., Pharris, A., Spiteri, G., Deogan, C., Suk, J. E., Soteriou, S., Papandreou, A., Silvestros, V., Athanasiadou, M., Kyprianou, T., Demetriou, A., Helve, O., Sarvikivi, E., Buda, S., Hauer, B., Haas, W., Wolff, T., Colgan, A., … Vergison, A. (2021). COVID-19 trends and severity among symptomatic children aged 0-17 years in 10 European Union countries, 3 August 2020 to 3 October 2021. *Eurosurveillance*, *26*(50), 1–8. https://doi.org/10.2807/1560-7917.ES.2021.26.50.2101098

Cohen, C. A., Li, A. P. Y., Hachim, A., Hui, D. S. C., Kwan, M. Y. W., Tsang, O. T. Y., Chiu, S. S., Chan, W. H., Yau, Y. S., Kavian, N., Ma, F. N. L., Lau, E. H. Y., Cheng, S. M. S., Poon, L. L. M., Peiris, M., & Valkenburg, S. A. (2021). SARS-CoV-2 specific T cell responses are lower in children and increase with age and time after infection. *Nature Communications*, *12*(1). https://doi.org/10.1038/s41467-021-24938-4

Dan, J. M., Lindestam Arlehamn, C. S., Weiskopf, D., da Silva Antunes, R., Havenar-Daughton, C., Reiss, S. M., Brigger, M., Bothwell, M., Sette, A., & Crotty, S. (2016). A Cytokine-Independent Approach To Identify Antigen-Specific Human Germinal Center T Follicular Helper Cells and Rare Antigen-Specific CD4 + T Cells in Blood . *The Journal of Immunology*, *197*(3), 983–993. https://doi.org/10.4049/jimmunol.1600318

Dan, J. M., Mateus, J., Kato, Y., Hastie, K. M., Yu, E. D., Faliti, C. E., Grifoni, A., Ramirez, S. I., Haupt, S., Frazier, A., Nakao, C., Rayaprolu, V., Rawlings, S. A., Peters, B., Krammer, F., Simon, V., Saphire, E. O., Smith, D. M., Weiskopf, D., … Crotty, S. (2021). Immunological memory to SARS-CoV-2 assessed for up to 8 months after infection. *Science*, *371*(6529). https://doi.org/10.1126/science.abf4063

Dong, Y., Dong, Y., Mo, X., Hu, Y., Qi, X., Jiang, F., Jiang, Z., Jiang, Z., Tong, S., Tong, S., & Tong, S. (2020). Epidemiology of COVID-19 among children in China. In *Pediatrics* (Vol. 145, Issue 6). American Academy of Pediatrics. https://doi.org/10.1542/peds.2020-0702

Dowell, A. C., Butler, M. S., Jinks, E., Tut, G., Lancaster, T., Sylla, P., Begum, J., Bruton, R., Pearce, H., Verma, K., Logan, N., Tyson, G., Spalkova, E., Margielewska-Davies, S., Taylor, G. S., Syrimi, E., Baawuah, F., Beckmann, J., Okike, I. O., … Ladhani, S. (2022). Children develop robust and sustained cross-reactive spike-specific immune responses to SARS-CoV-2 infection. *Nature Immunology*, *23*(1), 40–49. https://doi.org/10.1038/s41590-021-01089-8

Dowling, D. J., & Levy, O. (2014). Ontogeny of early life immunity. In *Trends in Immunology* (Vol. 35, Issue 7, pp. 299–310). Elsevier Ltd. https://doi.org/10.1016/j.it.2014.04.007

Elias, G., Ogunjimi, B., & Van Tendeloo, V. (2020). Activation-induced surface proteins in the identification of antigen-responsive CD4 T cells. In *Immunology Letters* (Vol. 219, pp. 1–7). Elsevier B.V. https://doi.org/10.1016/j.imlet.2019.12.006

Filippatos, F., Tatsi, E. B., & Michos, A. (2021). Immune response to SARS-CoV-2 in children: A review of the current knowledge. In *Pediatric Investigation* (Vol. 5, Issue 3, pp. 217–228). John Wiley and Sons Inc. https://doi.org/10.1002/ped4.12283

Garrido, C., Hurst, J. H., Lorang, C. G., Aquino, J. N., Rodriguez, J., Pfeiffer, T. S., Singh, T., Semmes, E. C., Lugo, D. J., Rotta, A. T., Turner, N. A., Burke, T. W., McClain, M. T., Petzold, E. A., Permar, S. R., Moody,

M. A., Woods, C. W., Kelly, M. S., & Fouda, G. G. (2021). Asymptomatic or mild symptomatic SARS-CoV-2 infection elicits durable neutralizing antibody responses in children and adolescents. *JCI Insight*, *6*(17). https://doi.org/10.1172/jci.insight.150909

Goldblatt, D., Alter, G., Crotty, S., & Plotkin, S. A. (2022). Correlates of protection against SARS - CoV -2 infection and COVID-19 disease . *Immunological Reviews*, 1–21. https://doi.org/10.1111/imr.13091

Grifoni, A., Sidney, J., Vita, R., Peters, B., Crotty, S., Weiskopf, D., & Sette, A. (2021). SARS-CoV-2 human T cell epitopes: Adaptive immune response against COVID-19. In *Cell Host and Microbe* (Vol. 29, Issue 7, pp. 1076–1092). Cell Press. https://doi.org/10.1016/j.chom.2021.05.010

Grifoni, A., Weiskopf, D., Ramirez, S. I., Mateus, J., Dan, J. M., Moderbacher, C. R., Rawlings, S. A., Sutherland, A., Premkumar, L., Jadi, R. S., Marrama, D., de Silva, A. M., Frazier, A., Carlin, A. F., Greenbaum, J. A., Peters, B., Krammer, F., Smith, D. M., Crotty, S., & Sette, A. (2020). Targets of T Cell Responses to SARS-CoV-2 Coronavirus in Humans with COVID-19 Disease and Unexposed Individuals. *Cell*, *181*(7), 1489-1501.e15. https://doi.org/10.1016/j.cell.2020.05.015

Hsieh, L. E., Grifoni, A., Sidney, J., Shimizu, C., Shike, H., Ramchandar, N., Moreno, E., Tremoulet, A. H., Burns, J. C., & Franco, A. (2022). Characterization of SARS-CoV-2 and common cold coronavirus-specific T-cell responses in MIS-C and Kawasaki disease children. *European Journal of Immunology*, *52*(1), 123–137. https://doi.org/10.1002/eji.202149556

Kaaijk, P., Pimentel, V. O., Emmelot, M. E., Poelen, M., Cevirgel, A., Schepp, R. M., den Hartog, G., Reukers, D. F. M., Beckers, L., van Beek, J., van Els, C. A. C. M., Meijer, A., Rots, N. Y., & de Wit, J. (2022). Children and Adults With Mild COVID-19: Dynamics of the Memory T Cell Response up to 10 Months. *Frontiers in Immunology*, *13*. https://doi.org/10.3389/fimmu.2022.817876

Lafon, E., Diem, G., Witting, C., Zaderer, V., Bellmann-weiler, R. M., Reindl, M., Bauer, A., Griesmacher, A., Fux, V., Hoermann, G., Miller, C., Zabernigg, A., Wöll, E., Wil, D., Lass-flörl, C., & Posch, W. (2021). *Potent SARS-CoV-2-Speci fi c T Cell Immunity and Low Anaphylatoxin Levels Correlate With Mild Disease Progression in COVID-19 Patients*. *12*(June), 1–14. https://doi.org/10.3389/fimmu.2021.684014

Liguoro, I., Pilotto, C., Bonanni, M., Ferrari, M. E., Pusiol, A., Nocerino, A., Vidal, E., & Cogo, P. (2020). SARS-COV-2 infection in children and newborns: a systematic review. *European Journal of Pediatrics*, *179*(7), 1029–1046. https://doi.org/10.1007/s00431-020-03684-7

Ludvigsson, J. F. (2020). Systematic review of COVID-19 in children shows milder cases and a better prognosis than adults. *Acta Paediatrica, International Journal of Paediatrics*, *109*(6), 1088–1095. https://doi.org/10.1111/apa.15270

Mansourian, M., Ghandi, Y., Habibi, D., & Mehrabi, S. (2021). COVID-19 infection in children: A systematic review and meta-analysis of clinical features and laboratory findings. *Archives de Pediatrie*, *28*(3), 242–248. https://doi.org/10.1016/j.arcped.2020.12.008

Mateus, J., Dan, J. M., Zhang, Z., Moderbacher, C. R., Lammers, M., Goodwin, B., Sette, A., Crotty, S., & Weiskopf, D. (2021). Low-dose mRNA-1273 COVID-19 vaccine generates durable memory enhanced by cross-reactive T cells. *Science*, *374*(6566). https://doi.org/10.1126/science.abj9853

Moderbacher, C. R., Ramirez, S. I., Dan, J. M., Smith, D. M., Sette, A., Moderbacher, C. R., Ramirez, S. I., Dan, J. M., Grifoni, A., & Hastie, K. M. (2020). Antigen-Specific Adaptive Immunity to SARS-CoV-2 in Acute COVID-19 and Associations with Age and Disease Severity ll Antigen-Specific Adaptive Immunity to SARS-CoV-2 in Acute COVID-19 and Associations with Age and Disease Severity. *Cell*, *183*(4), 996-1012.e19. https://doi.org/10.1016/j.cell.2020.09.038

Moss, P. (2022). The T cell immune response against SARS-CoV-2. *Nature Immunology*, *23*(2), 186–193. https://doi.org/10.1038/s41590-021-01122-w

Nelson, R. W., Chen, Y., Venezia, O. L., Majerus, R. M., Shin, D. S., Collection, M. G. H. C.-, Team, P., Carrington, M. N., Yu, X. G., Wesemann, D. R., Moon, J. J., & Luster, A. D. (2022). *SARS-CoV-2 epitope – specific CD4 + memory T cell responses across COVID-19 disease severity and antibody durability*. *9464*(July), 1–13.

Petrara, M. R., Bonfante, F., Costenaro, P., Cantarutti, A., Carmona, F., Ruffoni, E., Di Chiara, C., Zanchetta, M., Barzon, L., Donà, D., Da Dalt, L., Bortolami, A., Pagliari, M., Plebani, M., Rossi, P., Cotugno, N., Palma, P., Giaquinto, C., & De Rossi, A. (2021). Asymptomatic and Mild SARS-CoV-2 Infections Elicit Lower Immune Activation and Higher Specific Neutralizing Antibodies in Children Than in Adults. *Frontiers in Immunology*, *12*. https://doi.org/10.3389/fimmu.2021.741796

Qi, K., Zeng, W., Ye, M., Zheng, L., Song, C., Hu, S., Duan, C., Wei, Y., Peng, J., Zhang, W., & Xu, J. (2021). Clinical, laboratory, and imaging features of pediatric COVID-19. *Medicine*, *100*(15), e25230. https://doi.org/10.1097/md.0000000000025230

Reiss, S., Baxter, A. E., Cirelli, K. M., Dan, J. M., Morou, A., Daigneault, A., Brassard, N., Silvestri, G., Routy, J. P., Havenar-Daughton, C., Crotty, S., & Kaufmann, D. E. (2017). Comparative analysis of activation induced marker (AIM) assays for sensitive identification of antigen-specific CD4 T cells. *PLoS ONE*, *12*(10). https://doi.org/10.1371/journal.pone.0186998

Rowntree, L. C., Nguyen, T. H. O., Kedzierski, L., Neeland, M. R., Petersen, J., Crawford, J. C., Allen, L. F., Clemens, E. B., Chua, B., McQuilten, H. A., Minervina, A. A., Pogorelyy, M. V., Chaurasia, P., Tan, H.-X., Wheatley, A. K., Jia, X., Amanat, F., Krammer, F., Allen, E. K., … Kedzierska, K. (2022). SARS-CoV-2-specific T cell memory with common TCRαβ motifs is established in unvaccinated children who seroconvert after infection. *Immunity*. https://doi.org/10.1016/j.immuni.2022.06.003

Sekine, T., Perez-Potti, A., Rivera-Ballesteros, O., Strålin, K., Gorin, J. B., Olsson, A., Llewellyn-Lacey, S., Kamal, H., Bogdanovic, G., Muschiol, S., Wullimann, D. J., Kammann, T., Emgård, J., Parrot, T., Folkesson, E., Akber, M., Berglin, L., Bergsten, H., Brighenti, S., … Buggert, M. (2020). Robust T Cell Immunity in Convalescent Individuals with Asymptomatic or Mild COVID-19. *Cell*, *183*(1), 158-168.e14. https://doi.org/10.1016/j.cell.2020.08.017

Sette, A., & Crotty, S. (2022). Immunological memory to SARS-CoV -2 infection and COVID -19 vaccines . *Immunological Reviews*. https://doi.org/10.1111/imr.13089

Singh, V., Obregon-Perko, V., Lapp, S. A., Horner, A. M., Brooks, A., Macoy, L., Hussaini, L., Lu, A., Gibson, T., Silvestri, G., Grifoni, A., Weiskopf, D., Sette, A., Anderson, E. J., Rostad, C. A., & Chahroudi, A. (2022). Limited induction of SARS-CoV-2–specific T cell responses in children with multisystem inflammatory syndrome compared with COVID-19. *JCI Insight*, *7*(4). https://doi.org/10.1172/jci.insight.155145

Tan, A. T., Linster, M., Tan, C. W., Le Bert, N., Chia, W. N., Kunasegaran, K., Zhuang, Y., Tham, C. Y. L., Chia, A., Smith, G. J. D., Young, B., Kalimuddin, S., Low, J. G. H., Lye, D., Wang, L. F., & Bertoletti, A. (2021). Early induction of functional SARS-CoV-2-specific T cells associates with rapid viral clearance and mild disease in COVID-19 patients. *Cell Reports*, *34*(6), 108728. https://doi.org/10.1016/j.celrep.2021.108728

Tarke, A., Coelho, C. H., Zhang, Z., Dan, J. M., Yu, E. D., Methot, N., Bloom, N. I., Goodwin, B., Phillips, E., Mallal, S., Sidney, J., Filaci, G., Weiskopf, D., da Silva Antunes, R., Crotty, S., Grifoni, A., & Sette, A. (2022). SARS-CoV-2 vaccination induces immunological T cell memory able to cross-recognize variants from Alpha to Omicron. *Cell*, *185*(5), 847-859.e11. https://doi.org/10.1016/j.cell.2022.01.015

Tarke, A., Potesta, M., Varchetta, S., Fenoglio, D., Iannetta, M., Sarmati, L., Mele, D., Dentone, C., Bassetti, M., Montesano, C., Mondelli, M. U., Filaci, G., Grifoni, A., & Sette, A. (2022). Early and Polyantigenic CD4 T Cell Responses Correlate with Mild Disease in Acute COVID-19 Donors. *International Journal of Molecular Sciences*, *23*(13), 1–13. https://doi.org/10.3390/ijms23137155

Tarke, A., Sidney, J., Methot, N., Yu, E. D., Zhang, Y., Dan, J. M., Goodwin, B., Rubiro, P., Sutherland, A.,

Wang, E., Frazier, A., Ramirez, S. I., Rawlings, S. A., Smith, D. M., da Silva Antunes, R., Peters, B., Scheuermann, R. H., Weiskopf, D., Crotty, S., … Sette, A. (2021). Impact of SARS-CoV-2 variants on the total CD4+ and CD8+ T cell reactivity in infected or vaccinated individuals. *Cell Reports Medicine*, *2*(7), 100355. https://doi.org/10.1016/j.xcrm.2021.100355

Tian, X., Bai, Z., Cao, Y., Liu, H., Liu, D., Liu, W., & Li, J. (2022). Evaluation of Clinical and Immune Responses in Recovered Children with Mild COVID-19. *Viruses*, *14*(1). https://doi.org/10.3390/v14010085

Uzunoglu, S. S., & Akca, H. (2021). Systematic review: Clinical symptoms and laboratory and radiology findings in children with COVID-19. In *Nigerian Journal of Clinical Practice* (Vol. 24, Issue 9, pp. 1259–1267). https://doi.org/10.4103/njcp.njcp_577_20

Weisberg, S. P., Connors, T. J., Zhu, Y., Baldwin, M. R., Lin, W. H., Wontakal, S., Szabo, P. A., Wells, S. B., Dogra, P., Gray, J., Idzikowski, E., Stelitano, D., Bovier, F. T., Davis-Porada, J., Matsumoto, R., Poon, M. M. L., Chait, M., Mathieu, C., Horvat, B., … Farber, D. L. (2021). Distinct antibody responses to SARS-CoV-2 in children and adults across the COVID-19 clinical spectrum. *Nature Immunology*, *22*(1), 25–31. https://doi.org/10.1038/s41590-020-00826-9

Yoshida, M., Worlock, K. B., Huang, N., Lindeboom, R. G. H., Butler, C. R., Kumasaka, N., Dominguez Conde, C., Mamanova, L., Bolt, L., Richardson, L., Polanski, K., Madissoon, E., Barnes, J. L., Allen-Hyttinen, J., Kilich, E., Jones, B. C., de Wilton, A., Wilbrey-Clark, A., Sungnak, W., … Meyer, K. B. (2022). Local and systemic responses to SARS-CoV-2 infection in children and adults. *Nature*, *602*(7896), 321–327. https://doi.org/10.1038/s41586-021-04345-x

Yu, E. D., Wang, E., Garrigan, E., Goodwin, B., Sutherland, A., Tarke, A., Chang, J., Gálvez, R. I., Mateus, J., Ramirez, S. I., Rawlings, S. A., Smith, D. M., Filaci, G., Frazier, A., Weiskopf, D., Dan, J. M., Crotty, S., Grifoni, A., Sette, A., & da Silva Antunes, R. (2022). Development of a T cell-based immunodiagnostic system to effectively distinguish SARS-CoV-2 infection and COVID-19 vaccination status. *Cell Host and Microbe*, *30*(3), 388-399.e3. https://doi.org/10.1016/j.chom.2022.02.003

Zhang, Z., Mateus, J., Coelho, C. H., Dan, J. M., Moderbacher, C. R., Gálvez, R. I., Cortes, F. H., Grifoni, A., Tarke, A., Chang, J., Escarrega, E. A., Kim, C., Goodwin, B., Bloom, N. I., Frazier, A., Weiskopf, D., Sette, A., & Crotty, S. (2022). Humoral and cellular immune memory to four COVID-19 vaccines. *Cell*, 2434–2451. https://doi.org/10.1016/j.cell.2022.05.022

Zimmermann, P., & Curtis, N. (2022). Why Does the Severity of COVID-19 Differ With Age? Understanding the Mechanisms Underlying the Age Gradient in Outcome Following SARS-CoV-2 Infection. In *Pediatric Infectious Disease Journal* (Vol. 41, Issue 2, pp. E36–E45). Lippincott Williams and Wilkins. https://doi.org/10.1097/INF.0000000000003413